NOAA Atlas NESDIS 79

doi:10.7289/V5D21VM9

REGIONAL CLIMATOLOGY OF THE EAST ASIAN SEAS: AN INTRODUCTION

National Centers for Environmental Information
Silver Spring, Maryland

December 2015

U.S. DEPARTMENT OF COMMERCE
National Oceanic and Atmospheric Administration
National Environmental Satellite, Data, and Information Service

National Centers for Environmental Information

Additional copies of this publication, as well as information about National Centers for Environmental Information (formerly the National Oceanographic Data Center) data holdings and services, are available upon request directly from the National Centers for Environmental Information.

National Centers for Environmental Information
User Services Team
NOAA/NESDIS/NCEI
SSMC III, 4th floor
1315 East-West Highway
Silver Spring, MD 20910-3282

Telephone: (301) 713-3277
E-mail: NODC.Services@noaa.gov
NCEI Oceans Home Page: http://www.ncei.noaa.gov/

This document should be cited as:

Johnson, D.R., Boyer, T.P., 2015: Regional Climatology of the East Asian Seas: An Introduction. *NOAA Atlas NESDIS 79*, Silver Spring, MD, 37 pp. doi:10.7289/V5D21VM9.

This document is available at
http://data.nodc.noaa.gov/woa/REGCLIM/EAS/DOC/nesdis79-doi107289V5D21VM9.pdf.

Editor: Dan Seidov, National Centers for Environmental Information
Technical Editor: Alexey Mishonov, National Centers for Environmental Information

NOAA Atlas NESDIS 79
doi:10.7289/V5D21VM9

REGIONAL CLIMATOLOGY OF THE EAST ASIAN SEAS: AN INTRODUCTION

Daphne R. Johnson and Tim P. Boyer

National Centers for Environmental Information
Silver Spring, Maryland
December 2015

U.S. DEPARTMENT OF COMMERCE
Penny Pritzker, Secretary

National Oceanic and Atmospheric Administration
Kathryn Sullivan
Under Secretary of Commerce for Oceans and Atmosphere
and NOAA Administrator

National Environmental Satellite, Data, and Information Service
Stephen Volz, Assistant Administrator

This page intentionally left blank

Table of Contents

This page intentionally left blank

ABSTRACT

This paper describes the East Asian Seas Regional Climatology documenting spatial and temporal distribution of temperature and salinity on 1°, 1/4°, and 1/10° latitude-longitude grids. The temperature and salinity data fields used to generate these climatologies were computed by objective analysis of all quality-controlled data from the World Ocean Database 2013. High-resolution climatologies (especially 1/10°) reveal numerous meso-scale features such as water masses, fronts, and river outflows. These features are described in the context of the general oceanography of the study region and compared with *in situ* observations of the same features reported in the oceanographic literature. The feature-centric approach is shown to be a powerful instrument for validation of the East Asian Seas Regional Climatology and, by extension, of other regional climatologies.

1. INTRODUCTION

This paper describes main features of the East Asian Seas Regional Climatology (EAS-Regional Climatology; Johnson and Boyer, 2015), which is a product of collaboration between the National Oceanic and Atmospheric Administration / National Centers for Environmental Information (NOAA/NCEI), (formerly National Oceanographic Data Center, NODC), USA and the Ministry of Oceans and Fisheries / National Institute of Fisheries Science (MOF/NIFS), (formerly National Fisheries Research and Development Institute, NFRDI), Republic of Korea. The major objective of the EAS Regional Climatology project is to document temperature and salinity fields in temperate marginal seas bordering China, Taiwan, Korea, Japan and Russia. These include the East China Sea, Yellow Sea, Bohai Sea, Sea of Japan, northern Philippine Sea, and the adjacent Northwest Pacific Ocean. The study area (Figure 1.1) is 115°E to 143°E and 24°N to 52°N. The EAS Regional Climatology includes high-resolution maps (with 1/4° and 1/10° resolution) revealing some meso-scale features – fronts, quasi-stationary gyres/eddies, and river plumes – that were not resolved in previous climatologies with coarser resolutions.

The EAS Regional Climatology is part of a series of regional climatologies developed at the NCEI (Boyer *et al*., 2012; Seidov *et al*., 2013; Boyer *et al*., 2015; Seidov *et al*., 2015).

Physical parameters analyzed for this climatology are temperature and salinity for the time period of 1804 to 2013. Fields used to generate this climatology were computed by objective analysis of all quality-controlled data from the World Ocean Database 2013. These data are available from the NCEI and World Data Center (WDC) for Oceanography, Silver Spring, Maryland.

This paper is structured as follows. First, the oceanography of each marginal sea and adjacent Northwest Pacific Ocean is described (Section 2), followed by data and methods (Section 3), results (Section 4), availability of maps and data (Section 5), summary (Section 6), acknowledgments (Section 7), and references (Section 8).

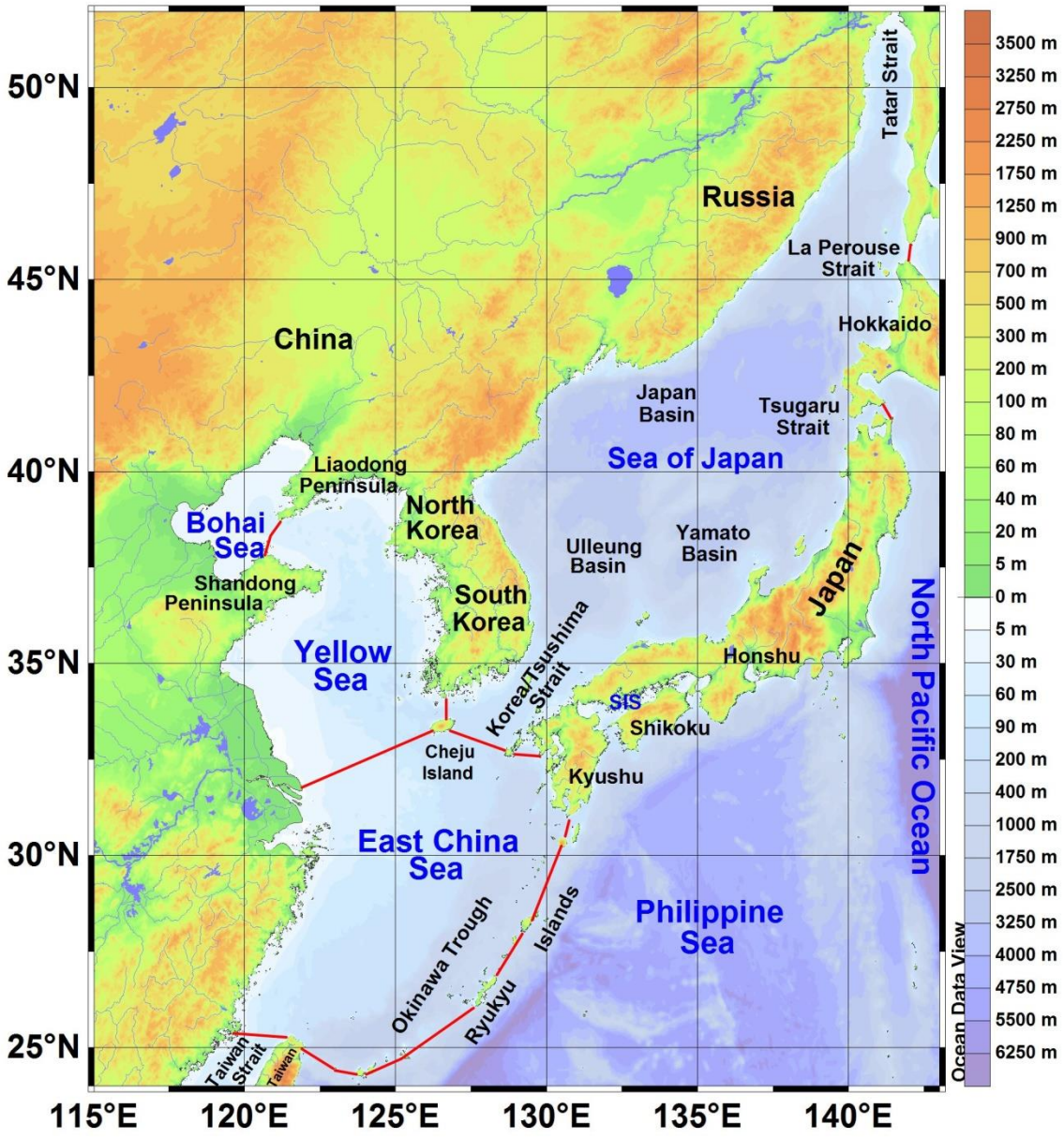

Figure 1.1. Base map of the East Asian Seas. Bathymetry: ETOPO1 (Amante and Eakins, 2009). Boundaries are adapted from International Hydrographic Organization (1953) with minor modifications. SIS, Seto Inland Sea.

2. OCEANOGRAPHY OF EAST ASIAN SEAS

Property distributions in the EAS are controlled by ocean-atmosphere interaction, tides, river outflows, and currents interconnecting these seas and linking them to the adjacent Northwest Pacific Ocean and the Philippine Sea through several straits (Figure 1.1). The main circulation features that impact horizontal and vertical water-mass structure are inflows and outflows through these straights as well as quasi-stationary gyres.

2.1 EAST CHINA SEA

The East China Sea is located between China, Taiwan, Japan, and South Korea. Main water bodies around the East China Sea are the Yellow Sea in the north, Korea/Tsushima Strait and Sea of Japan in the northeast, Philippine Sea in the east, and Taiwan Strait and South China Sea in the south. The East China Sea area is 752,000 km^2 (Belkin, 2002a). The sea is mostly shallow: continental shelf with depths less than 150 m occupies three quarters of the sea. Only in the Okinawa Trough, west of the Ryukyu Islands, the ocean depth exceeds 2000 m. The East China Sea Shelf combined with the adjacent Yellow and Bohai Seas forms the largest shelf in the Pacific Ocean with the total area of 900,000 km^2, making it one of the World Ocean's largest shelves (Belkin, 2002a).

The climate and oceanographic regime of the East China Sea depend largely on the East Asian Monsoon and the Siberian High, a quasi-stationary high-pressure anticyclonic atmospheric system over northern Asia (Wu and Wang, 2002). In winter, monsoon winds from the north and northeast dominate the East China Sea, bringing cold, dry air. In summer, southerly and southwesterly winds prevail, bringing warm, moist air. The seasonally-reversing monsoon winds result in a bi-modal, distinctly seasonal circulation pattern in the East China Sea-Yellow Sea (ECS-YS) region (Figure 2.1; Su, 1998; Ichikawa and Beardsley, 2002); these monsoons are responsible for the wide range of sea surface temperature (SST) in the East China Sea. In winter, the Siberian cold air outbreaks result in tremendous ocean heat loss and convection that cool down the entire water column below 10°C, while in summer the upper mixed layer warms up to 28°C (Belkin, 2002a; Chen, 2009). The seasonal range of SST in the East China Sea thus exceeds 18°C, less than that in the Yellow Sea, yet still one of the largest seasonal SST ranges in the World Ocean. The Kuroshio Front's surface manifestation in SST is strongest in winter and almost absent in summer (Hickox *et al*., 2000).

The East China Sea receives up to 1000 km^3/yr of fresh water from the Yangtze River (Shen *et al*., 2013; Yang *et al*., 2014, 2015), resulting in low salinity water (<30) extending far offshore from the Yangtze River estuary (Beardsley *et al*., 1985; Chen, 2009; Li *et al*., 2012). Typically, the Yangtze River outflow extends southeast and south (Ichikawa and Beardsley, 2002; Chen, 2009); however, after major floods, the low-salinity plume occasionally extends eastward across the entire East China Sea and continues via the Korea/Tsushima Strait (Senjyu *et al*., 2006) into the Sea of Japan. The Yangtze River discharge decreased steadily in the long-term, especially after 1998 (Yang *et al*., 2010, 2014, 2015).

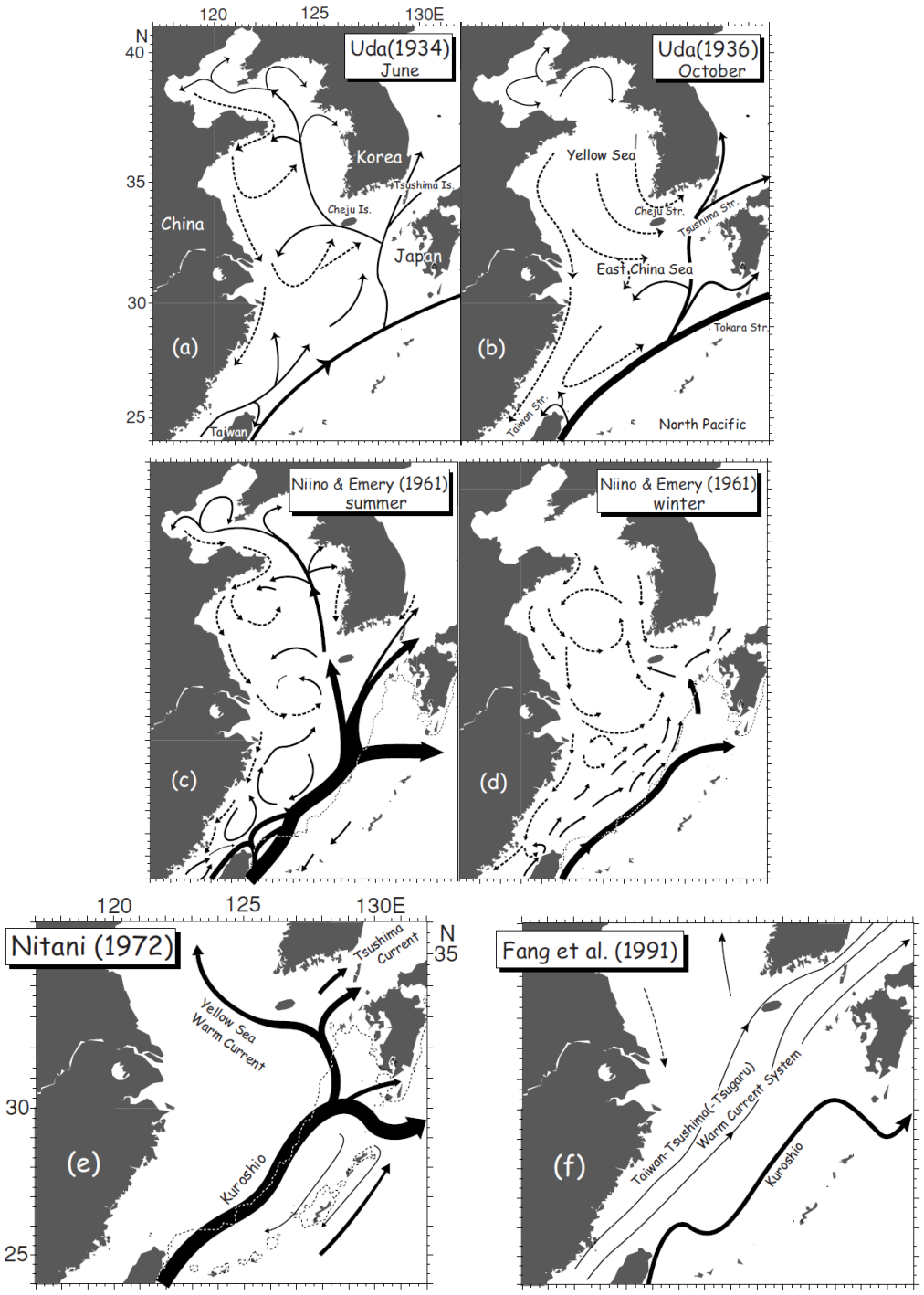

Figure 2.1. Circulation schematics of the ECS-YS region. After Isobe (2008, Fig. 1 and references therein; reproduced with permission from the Oceanographic Society of Japan). Solid/broken arrows show warm/cold currents in Uda (1934, 1936) and Fang *et al.* (1991). Solid/broken arrows in Niino and Emery (1961) show warm-saline/cool-fresh currents. Dotted line, 200 m isobath.

Various circulation schematics were proposed for the ECS-YS region (Figure 2.1). One of the most detailed circulation schematics (Ichikawa and Beardsley, 2002) is shown in Figure 2.2 discussed below.

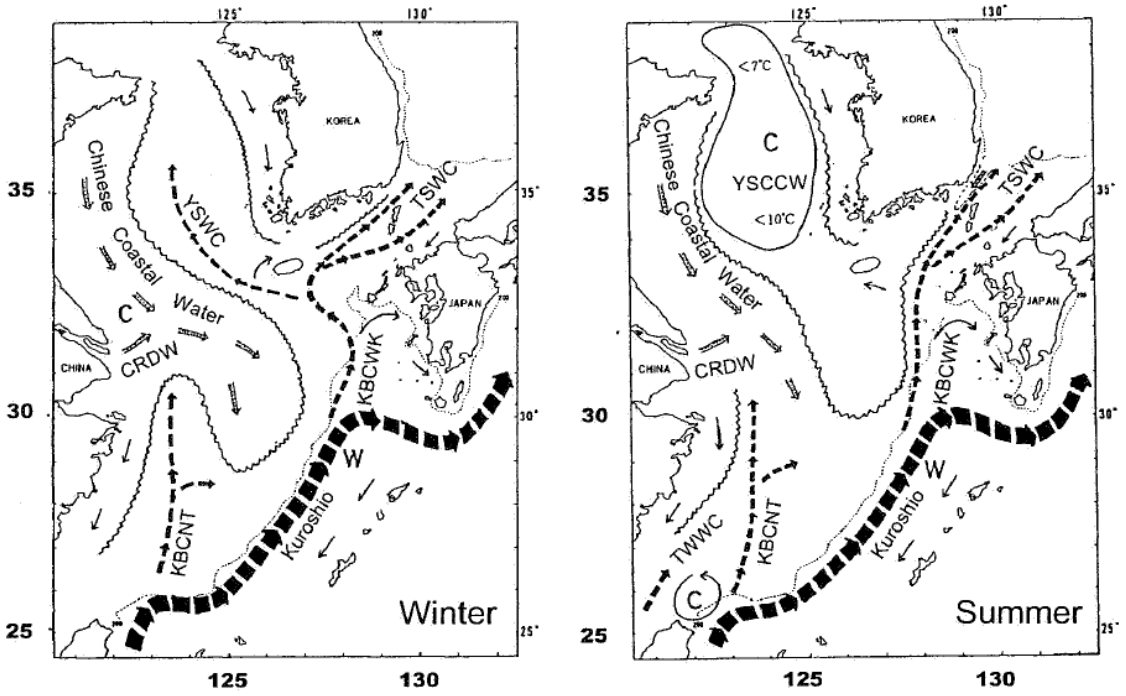

Figure 2.2. Winter (left) and summer (right) circulation near 50 m depth in the ECS-YS region after Ichikawa and Beardsley (2002), Fig. 6; reproduced with permission from the Oceanographic Society of Japan). Also shown are water masses and fronts (*ibid.*, after Kondo, 1985). Acronyms: CRDW, Changjiang River Diluted Water; KBCNT, Kuroshio Branch Current north of Taiwan; KBCWK, Kuroshio Branch Current west of Kyushu; TSWC, Tsushima Warm Current; TWWC, Taiwan Warm Current; YSCCW, Yellow Sea Central Cold Water; YSWC, Yellow Sea Warm Current. Dotted line, 200 m isobath.

The general circulation of the East China Sea is cyclonic (counterclockwise) and determined largely by the cold southward China Coastal Current and warm northward Kuroshio Current, Tsushima Current, and Taiwan Current (Lie and Cho, 1994; Su, 1998; Belkin, 2002a; Chen, 2009; Matsuno *et al.*, 2009). The China Costal Current carries relatively fresh and cold water from the Yellow Sea towards Taiwan Strait and eventually to the South China Sea (Jan *et al.*, 2002; Chen, 2009). The Taiwan Current brings salty and warm water from the South China Sea to the East China Sea through the Taiwan Strait (Su, 1998; Jan *et al.*, 2002; Chen, 2009). This water merges with the Yangtze River discharge and flows through the Korea/Tsushima Strait to the Sea of Japan. A branch of the Taiwan Current extends into the Yellow Sea. The Kuroshio Current flows along the shelf break – and sometimes over the outer shelf – and continues through the Tokara Strait south of Kyushu Island. The Tsushima Current flows across the East China Sea Shelf toward the Korea/Tsushima Strait where it enters the Sea of Japan (Lie and Cho, 1994; Belkin, 2002a; Chen, 2009; Matsuno *et al.*, 2009).

The East China Sea features numerous fronts of diverse nature: Kuroshio Front, Yangtze Bank Ring Front, Zhejiang-Fujian Front (China Coastal Current Front), tidal mixing fronts, and coastal upwelling fronts, while the Yellow and Bohai Seas feature mostly tidal mixing fronts (Figure 2.3; Hickox *et al.*, 2000; Belkin and Cornillon, 2003; Belkin *et al.*, 2009; Chen, 2009). These fronts are seasonally-persistent as they form at the same locations each year, during the same season, and are best defined in winter months, from January through March. Our high-resolution (1/10°) climatology (Section 4) resolved all major meso-scale fronts in this area, *e.g.*, the Shandong Peninsula, Jiangsu, Seohan Bay, and Kyunggi Bay fronts (Figure 2.3).

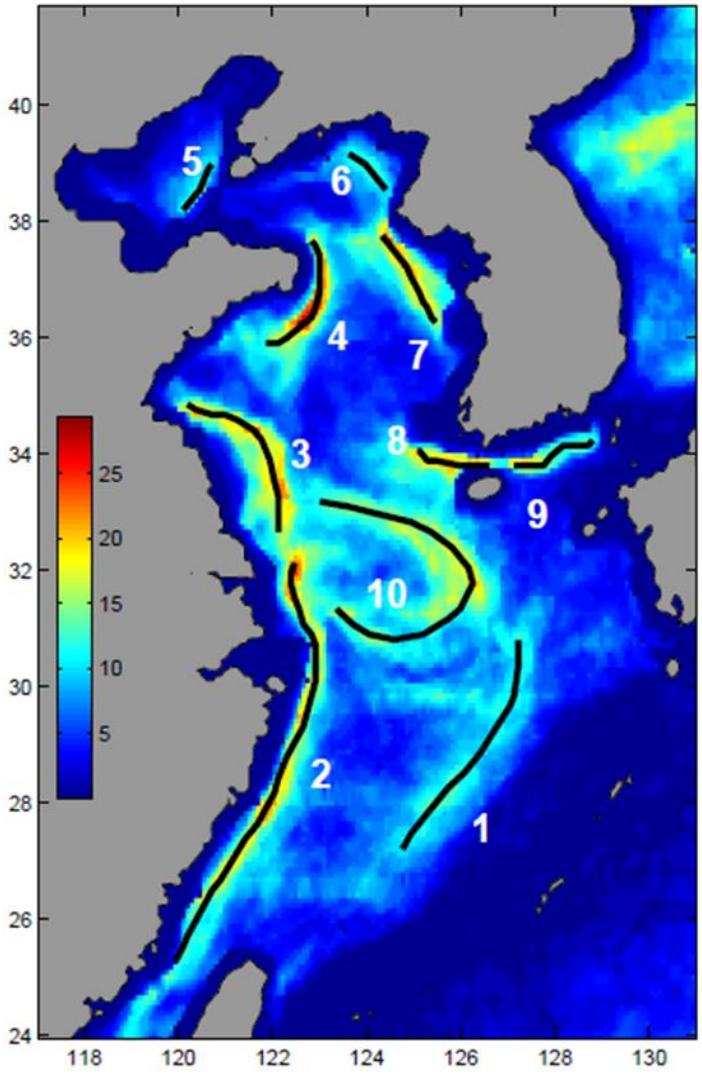

Figure 2.3. SST fronts of the East China, Yellow, and Bohai Seas (Hickox *et al.*, 2000, Fig. 2; reproduced with permission from the American Geophysical Union). Shown is long-term annual mean pixel-based frequency (%) of SST fronts based on 9-km resolution Pathfinder twice-daily fields, 1985-1996. For each 9-km pixel, shown is the percentage of total time that the given pixel contained a front, normalized on cloudiness. Black lines mark most frequent locations of fronts. Numbers are: 1, Kuroshio Front; 2, Zhejiang-Fujian Front; 3, Jiangsu Front; 4, Shandong Peninsula Front; 5, Bohai Sea Front; 6, Seohan Bay Front; 7, Kyunggi Bay Front; 8, Western Chejudo Front; 9, Eastern Chejudo Front; 10, Yangtze Bank Ring Front.

2.2 YELLOW SEA

The Yellow Sea is located between the Korean Peninsula in the east and China in the west. It borders the Bohai Sea (Gulf of Bohai) in the north and the East China Sea in the south. The Bohai Sea is often considered a part of the Yellow Sea. The boundary between the Yellow and East China Seas is defined here as a line connecting Cheju Island and the north bank of the Yangtze River (Changjiang) mouth (Teng *et al.*, 2005), so that the Yangtze River flows into the East China Sea. The Yellow Sea area (including the Bohai Sea) is 417,000 km^2 (Belkin, 2002b). The Yellow Sea is situated entirely over the continental shelf and has an average depth of 44 m (without the Bohai Sea) and maximum depth of 130 m (KORDI, 1987; Chen, 2009).

The Yellow Sea climate is driven by seasonal monsoons and is strongly affected by the Siberian High. In winter, cold air outbreaks from Siberia cause strong ocean-atmosphere interaction and rapid heat loss by the sea, followed by thermal convection and vigorous mixing. These processes often lead to complete vertical mixing and cooling of the entire water column below 10°C, down to <9°C in the central part of the Sea and down to <8°C in the northern part of the Sea (Zhang *et al.*, 2008). In summer, this cold water mass is capped by the seasonal thermocline, which can be quite sharp. For example, in mid-July 1997 Zhang *et al.* (2008) observed the upper mixed layer above the thermocline being warmer than 25°C while the water immediately beneath the thermocline remained colder than 8°C. Owing to severe winters and hot summers, the seasonal SST range is extremely wide, from 4°C in winter to 25°C in summer. Thermal fronts around the Yangtze Bank/Shoal, off Jiangsu Shoal, around Shandong Peninsula, and west of Seohan Bay and Kyunggi Bay are generated mostly by tidal mixing (Figure 2.3; Hickox *et al.*, 2000; Belkin and Cornillon, 2003; Belkin *et al.*, 2009; Chen, 2009).

The salinity field features a pronounced low-salinity region in the western part of the sea, with sea surface salinity (SSS) as low as 30, due to the enormous freshwater discharge of the Yangtze River, up to 1000 km^3/yr (Yang *et al.*, 2010, 2014, 2015), that flows into the adjacent East China Sea and also affects the Yellow Sea. The salinity of the Yellow Sea is also affected by the inflow of relatively saline waters transported northward by the Taiwan Current and Tsushima Current, the latter being the western branch of the Kuroshio Current (Figure 2.2; Ichikawa and Beardsley, 2002).

2.3 BOHAI SEA

The Bohai Sea is the smallest and shallowest of the four East Asian Seas, with an area of 77,000 km^2, volume of 1390 km^3, mean depth of 18 m and maximum depth of 30 m (Lin *et al.*, 2006; Chen, 2009). The sea is adjacent to two countries, China and North Korea, and is often considered an embayment of the Yellow Sea and called the Gulf of Bohai. The Bohai Sea exchanges water with the Yellow Sea, although the exchange is constricted by the Shandong Peninsula and the Liaodong Peninsula (Lin *et al.*, 2006). The proximity to Siberia makes the Bohai Sea climate harsher than the climates of other East Asian Seas. In winter, air temperature drops to -10°C (Teng *et al.*, 2005), SST decreases to <-1°C (Chen, 2009), and salinity decreases to <31 (Chen, 2009), with extensive sea ice cover forming during severe winters (Su and Wang, 2012; Yuan *et al.*, 2012). The summer climate is warm, with air temperatures up to 30°C (Teng *et al.*, 2005), SST up to 27°C, and salinity below 31.5 (Chen, 2009). The Bohai Sea is vertically homogeneous in winter, being stirred by winds, waves, tides and thermal convection (Lin *et al.*, 2006; Wang *et al.*, 2008). The sea is also relatively uniform horizontally with a single temperature front cutting across the central part of the sea (Hickox *et al.*, 2000).

The sea receives fresh water from the Yellow River (Huanghe) as well as a few smaller rivers (Hai, Liao, and Luan Rivers). The Yellow River runoff decreased dramatically over the last few decades (Yu *et al.*, 2013), resulting in an increase in the Bohai Sea salinity (Mao *et al.*, 2008). The Yellow River carries an enormous amount of sediments, 1600 Mt/yr (Taniguchi *et al.*, 2008), approximately three times the sediment flux of the Yangtze River in the 1950s-1960s and 11 times its present flux of 145 Mt/yr (Milliman and Meade, 1983; Yang *et al.*, 2014, 2015). The relatively small and shallow Bohai Sea is surrounded by densely populated and heavily industrialized coastal areas with a high level of urban, agricultural and industrial effluents that pollute the sea and cause severe eutrophication and harmful algae blooms (Tang *et al.*, 2006).

2.4 SEA OF JAPAN

The Sea of Japan is the largest and deepest of the four East Asian Seas, with an area of 1.013×10^6 km^2, mean depth of 1,667 m (Menard and Smith, 1966), and maximum depth of 3,700 m (Gamo *et al.*, 1986). It is bordered by Japan, Russia, North Korea, and South Korea. It is connected to the Okhotsk Sea in the north – via the Tatar Strait (Gulf of Tartary) and Nevelskoy Strait between mainland Russia and Sakhalin Island – and in the northeast via the La Perouse Strait (Soya Strait) between Sakhalin and Hokkaido. The Nevelskoy Strait is narrow and shallow (minimum depth about 10 m) yet it serves as a conduit for the southward branch of the Amur River outflow, which makes the Tatar Strait relatively fresh and feeds the Liman Current flowing southward along the Russian coast. The Sea of Japan's only connection with the open Pacific Ocean is via the Tsugaru Strait between Hokkaido and Honshu. In the south, the Sea of Japan is connected with the East China Sea via the Korea/Tsushima Strait. The Tsushima Current flows through the Korea/Tsushima Strait, carrying warm and salty waters from the East China Sea to the Sea of Japan.

The winter climate of the northern Sea of Japan is severe owing to the proximity to Siberia, with cold air outbreaks causing huge heat loss, cooling, and vigorous thermal convection, which is particularly intense off Peter the Great Bay centered at approximately 40.6° N, 131.8° E (Seung and Yoon, 1995; Nof, 2001; Talley *et al.*, 2003). The influx of cold ice-laden waters from the Okhotsk Sea with the Liman Current (Martin and Kawase, 1998) also contributes to the harshness of the local climate.

The southern Sea of Japan has a milder climate thanks to warm water influx from the East China Sea. The Sea of Japan is thus a meeting place of cold and fresh subarctic waters and warm and salty subtropical waters that converge to form the Polar Front (Isoda *et al.*, 1991; Belkin and Cornillon, 2003), also known as the Subpolar or Subarctic Front (Senjyu, 1999). This front extends zonally along 39-40°N, effectively separating the Sea of Japan into two oceanographic regions with distinct circulation regimes, sometimes referred to as the subarctic circulation in the north and subtropical circulation in the south (Senjyu, 1999).

The Sea of Japan circulation is structurally and dynamically complex (Figure 2.4) owing to (a) inflows and outflows through four straits (Korea/Tsushima, Tsugaru, La Perouse/Soya, and Tatar); (b) strong seasonal variability; (c) interaction between cold subarctic and warm subtropical waters; and (d) rugged topography, especially in the southern part of the sea, which facilitates formation of meso-scale eddies and quasi-stationary gyres.

The circulation in the southern Sea of Japan is formed by the northward Tsushima Current that splits into three branches after passing the Korea/Tsushima Strait. The westernmost

branch – East Korean Warm Current (EKWC) – flows northward along the Korean Peninsula's east coast, then turns to the northeast. The circulation in the northern and western Sea of Japan is dominated by the Liman Cold Current-North Korean Cold Current (LCC-NKCC in Figure 2.4), which flows southward along the Russian and Korean coasts (Yoon, 1982; Senjyu, 1999).

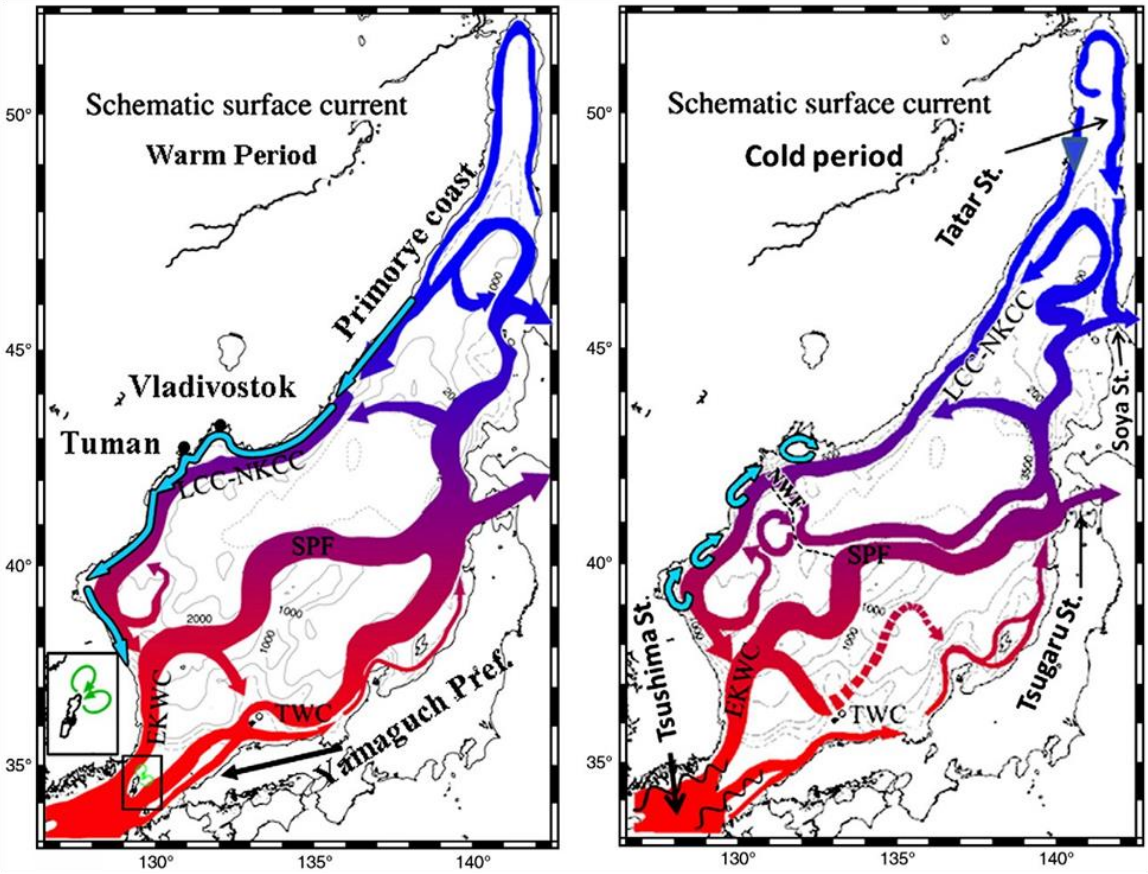

Figure 2.4. Schematic of surface circulation of the Sea of Japan during the warm (left) and cold (right) periods, corresponding to summer/winter monsoons respectively (Kim, 2007; after Yoon and Kim, 2009; reproduced with permission from Elsevier). Acronyms: EKWC, East Korean Warm Current; LCC–NKCC, Liman Cold Current–North Korean Cold Current; NWF, Northwest Front; SPF, Subpolar Front; TWC, Tsushima Warm Current.

A unique feature of the Sea of Japan is the formation of a deep water mass called the Japan Sea Proper Water (JSPW). The JSPW consists of two vertically-stacked water masses separated by a discontinuity at ~2000 m (Gamo *et al*., 1986; Sudo, 1986; Senjyu and Sudo, 1994; Seung and Yoon, 1995; Yoshikawa *et al*., 1999; Talley *et al*., 2006). The deep water mass (also called Bottom Water or Lower Japan Sea Proper Water) has an extremely low potential temperature of 0.0-0.2°C, a very narrow salinity range of 34.06-34.07, and a dissolved oxygen range of 220-230 μmol kg^{-1} (Gamo *et al*., 1986). The JSPW is formed by the wintertime deep convection south of Vladivostok (Senjyu and Sudo, 1993, 1994; Seung and Yoon, 1995; Choi, 1996; Senjyu, 1999).

No major river flows to the Sea of Japan whose salinity is controlled by precipitation/evaporation, saltwater import by the Tsushima Current and freshwater import by the Liman Current (Senjyu, 1999). Occasionally, after exceptionally massive floods, the Yangtze River Diluted Water (YRDW; standard term used by Chinese oceanographers) spreads through the Korea/Tsushima Strait into the Sea of Japan. Due to the long-term decrease in discharge of the Yellow River and Yangtze River caused mostly by the diversion of freshwater for agricultural use (Yang *et al.*, 2010, 2014, 2015; Yu *et al.*, 2013), salinity of the Sea of Japan is expected to increase, which could facilitate the development of deep convection and renewal of the Sea of Japan Bottom Water (Nof, 2001).

The rugged bathymetry of the southern Sea of Japan contributes to eddy formation, including intrathermocline eddies (Hogan and Hurlburt, 2006). The largest positive bathymetric feature here is the Yamato Rise (depth < 1000 m) (Kim *et al.*, 2004) surrounded by three deep basins: the Japan Basin in the north (depth > 3,500 m), the Yamato Basin (2,500-3,500 m) in the southeast, and the Ulleung (Tsushima) Basin (1,500-2,500 m) in the southwest.

2.5 Connection to the Philippine Sea and Northwest Pacific Ocean

The main circulation link between the Northwest Pacific Ocean, Philippine Sea, and East Asian Seas is the Kuroshio Current, which originates as the northward branch of the North Equatorial Current (Kawai, 1998; Qiu, 2001; Talley *et al.*, 2011; Figure 2.5 from Imawaki *et al.*, 2013). The main branch of the Kuroshio flows toward Japan, then south of Japan, leaving the coast off Cape Inubo (35°42´N, 140°52´E) to head eastward along 34°N to 35°N as the Kuroshio Extension. While flowing south of Honshu, the Kuroshio occasionally forms the so-called "Kuroshio Large Meander" that persists for many months. Two other quasi-stationary meanders (called the First and Second Kuroshio Meander) form downstream of Cape Inubo. These meanders are important for fisheries, marine transportation and other human activities.

The Oyashio Current (an extension of the southward East Kamchatka Current) flows southward along the east coasts of Hokkaido and Honshu down to about 40°N, where it sharply turns northeast and continues along the Polar Front (Belkin *et al.*, 2002). The broad 500-600 km zone between the cold, fresh Oyashio and warm, salty Kuroshio is one of the most dynamic frontal zones in the World Ocean, with winter SST ranging from 3°C in the north to 18°C in the south and spring SST ranging from 6°C to 21°C between the same locations. Owing to the vigorous mixing and water mass transformation in-between these fronts, this region is called the Kuroshio-Oyashio Transition Zone or the Mixed Water Region (Qiu, 2001; Figure 2.5 from Imawaki *et al.*, 2013). In the middle of this zone, the Subarctic Front extends eastward along 40°N (not shown in Fig. 2.5). The entire Kuroshio-Oyashio Mixed Water Region is filled with numerous warm (anticyclonic; clockwise) and cold (cyclonic; counterclockwise) rings spawned by meanders of the aforementioned currents and fronts.

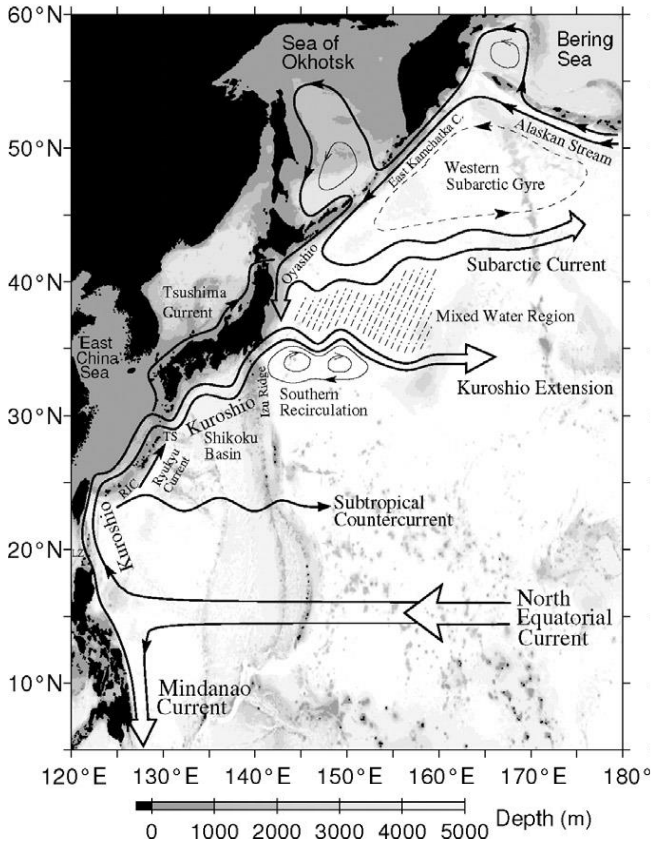

Figure 2.5. Circulation of the western North Pacific Ocean (Imawaki *et al.*, 2013, Fig. 13.12; reproduced with permission from Elsevier). Acronyms: LZ, Luzon Strait, RIC, Ryukyu Island Chain, TS, Tokara Strait.

3. DATA AND METHODS

The EAS Regional Climatology was developed using data from the most recent edition of the World Ocean Database (WOD13; Boyer *et al.*, 2013), which is freely available online from the NCEI Regional Climatology website.

Temperature and salinity data are from instrument files designated by NCEI as Ocean Station Data (OSD), Mechanical Bathythermographs (MBT), Expendable Bathythermographs (XBT), ship-deployed Conductivity-Temperature-Depth (CTD) probes, profiling floats (PFL), moored (MRB) and drifting buoys (DRB), and gliders (GLD); additionally, surface-only data collected by various platforms are used (SUR).

Figure 3.1 and Figure 3.2 show spatial distributions of temperature and salinity at 0 m, 30 m, 50 m, and 100 m. Figure 3.3 shows distributions of temperature (top) and salinity (bottom) vertical profiles by instrument type. There are 1.2 million temperature profiles and approximately 0.6 million salinity profiles covering the period of 1804-2013.

Long-term mean annual, seasonal, and monthly climatologies were calculated for the above period. Seasons are defined as: winter (January-March), spring (April-June), summer (July-September), and fall (October-December).

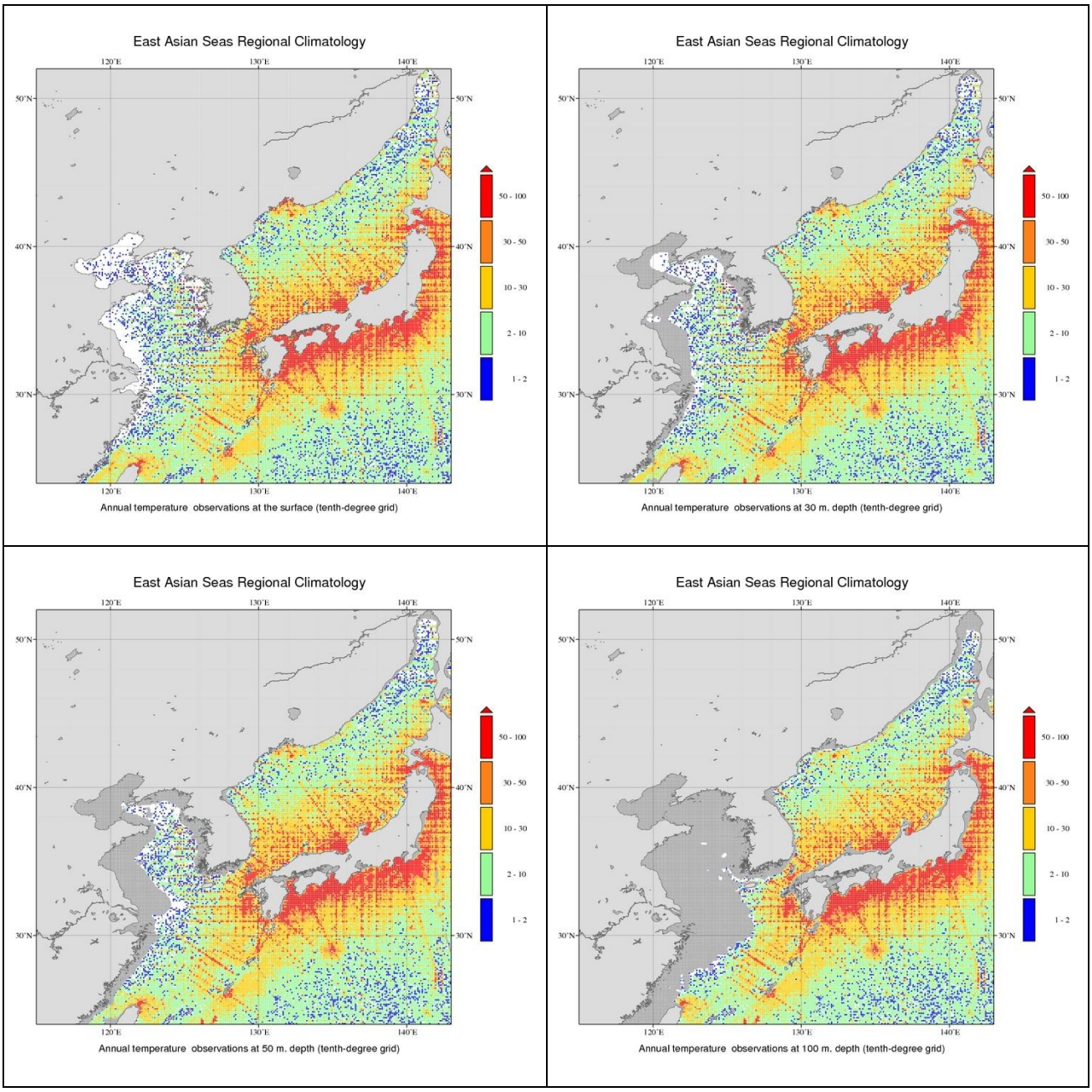

Figure 3.1. Distribution of temperature data at four depths (0, 30, 50, and 100 m) on the 1/10° grid. Shown are numbers of observations in each grid cell.

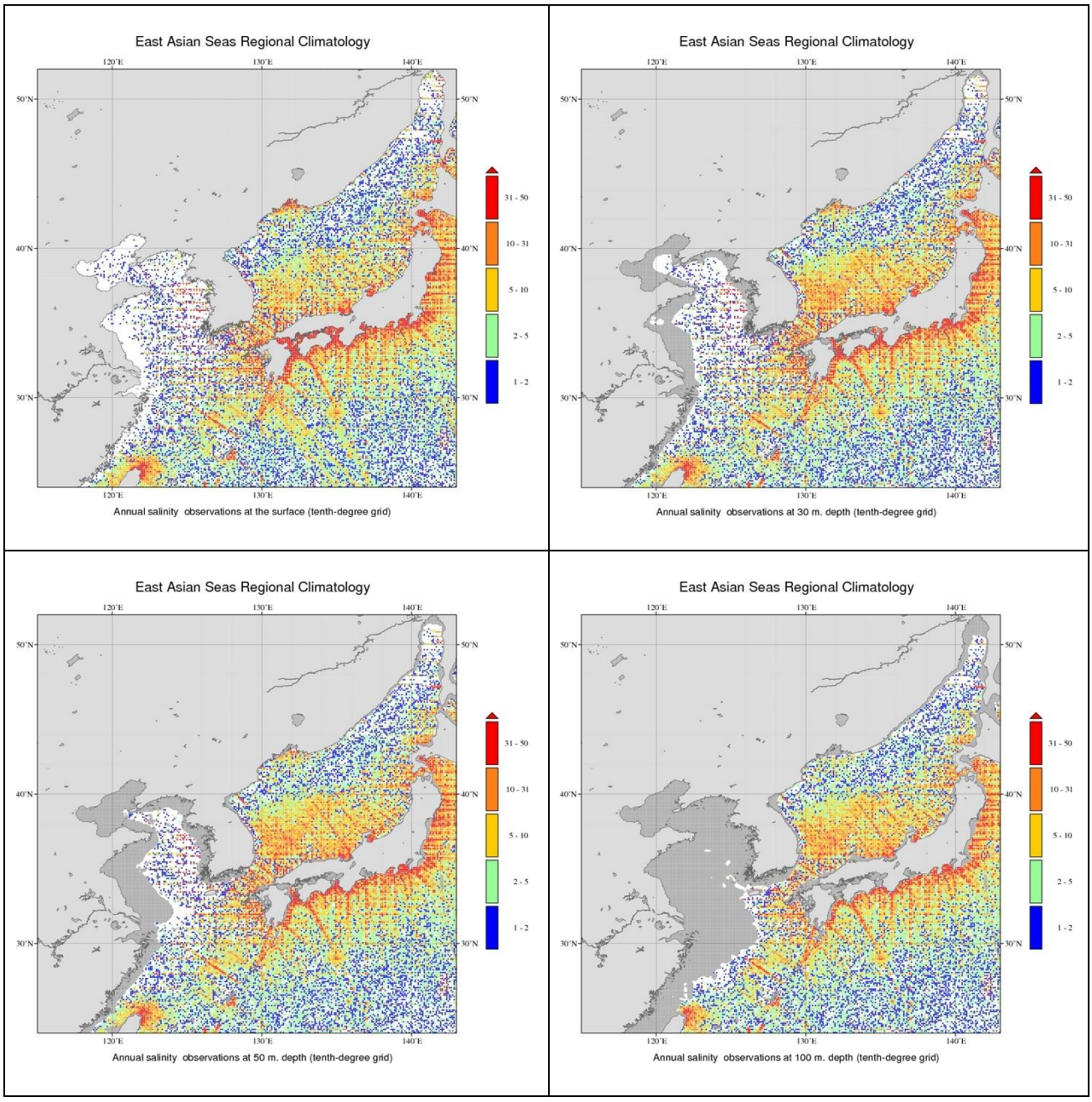

Figure 3.2. Distribution of salinity data at four depths (0, 30, 50, and 100 m) on the 1/10° grid. Shown are numbers of observations in each grid cell.

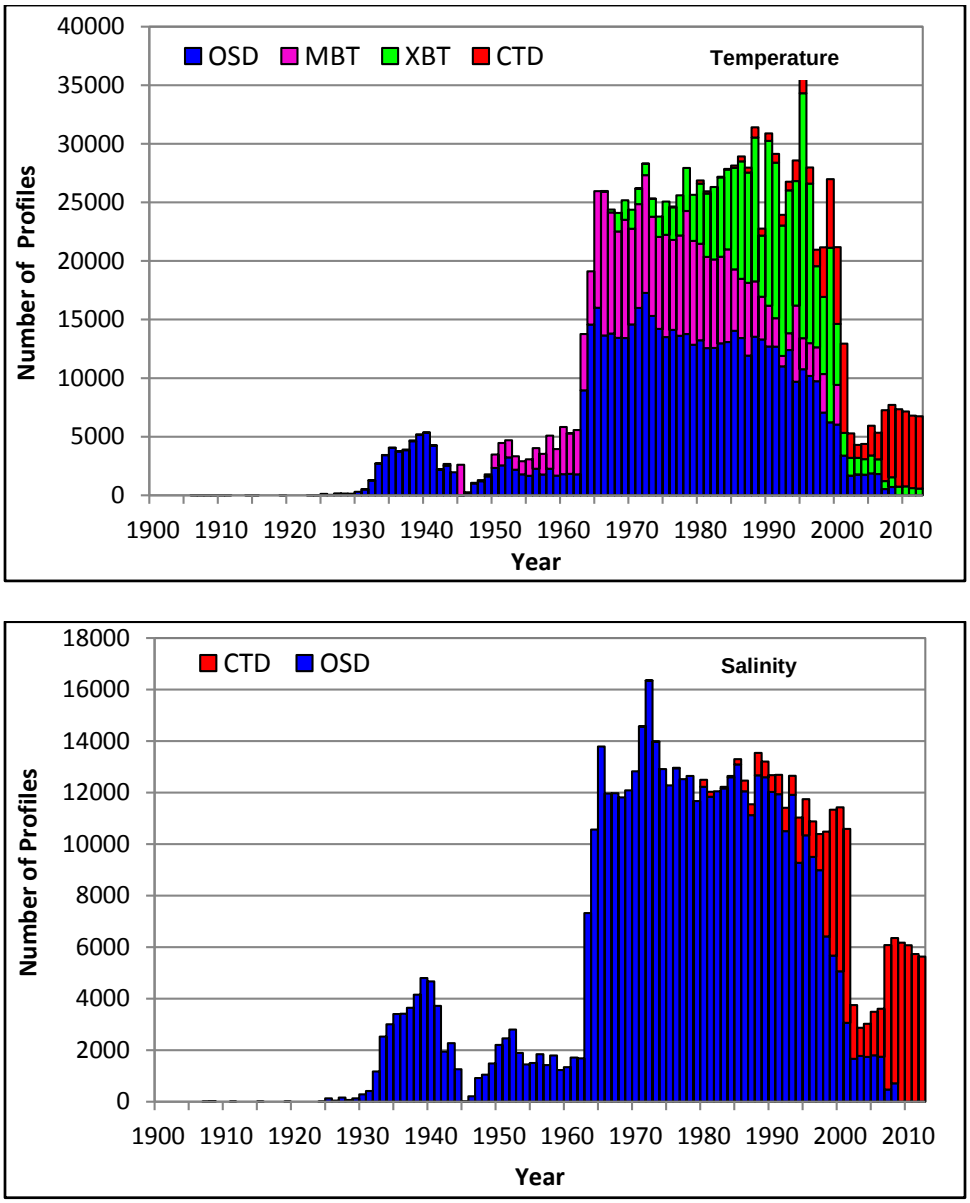

Figure 3.3. Distribution of temperature (top) and salinity (bottom) vertical profiles by instrument type and year. There are very few data from 1804-1899 (not shown). Acronyms: OSD, Ocean Station Data; CTD, Conductivity-Temperature-Depth probe; XBT, Expendable Bathythermograph; MBT, Mechanical Bathythermograph. For details about instrument types see Johnson *et al.* (2013).

The methods used in preparation of this climatology are similar to those employed to generate the World Ocean Atlases and NCEI Regional Climatologies (Locarnini *et al.* (2013) for temperature and Zweng *et al.* (2013) for salinity). Maps of temperature and salinity are available on 1°, 1/4°, and 1/10° latitude-longitude grids. The radius of influence varies with grid resolution from 892 km to 154 km respectively (Table 1) (see also Boyer *et al.*, 2005). Additional details on climatological calculations are found in Boyer *et al.* (2005, 2013).

Maps of temperature and salinity are available on 102 newly-defined standard levels for annual and seasonal fields and on 57 newly-defined standard levels for monthly fields (Table 2). For complete lists of these levels see Johnson *et al.* (2013). These new sets of standard levels

provide a substantially better vertical resolution than the standard levels used in the previous releases of World Ocean Atlases up to 2009. Annual and seasonal fields were calculated from the surface to 5500 m depth, while monthly fields were calculated from the surface to 1500 m depth.

Temperature is in degrees of Celsius (°C). Salinity is dimensionless.

Table 1. Radii of influence used in the objective analysis for 1°, 1/4°, and 1/10° climatologies.

Pass Number	1° Radius of Influence (km)	1/4° Radius of Influence (km)	1/10° Radius of Influence (km)
1	892	321	211
2	669	267	155
3	446	214	111

Table 2. Standard levels and datasets used in climatologies.

Oceanographic Variable	Standard Levels for Annual and Seasonal Climatology	Standard Levels for Monthly Climatology	Datasets Used to Calculate Climatology
Temperature	0-5500 m (102 levels)	0-1500 m (57 levels)	OSD, CTD, MBT, XBT, SUR, MRB, PFL, DRB, GLD
Salinity	0-5500 m (102 levels)	0-1500 m (57 levels)	OSD, CTD, SUR, MRB, PFL, DRB, GLD

4. CLIMATOLOGIES WITH DIFFERENT RESOLUTIONS

In this section we illustrate three climatologies with different spatial resolution, from the coarse 1° to the intermediate 1/4° to the fine 1/10° climatology. The highest spatial resolution of 1/10° demonstrates a major improvement in resolving various features of importance such as fronts, river plumes, and cold pools. Additionally, data quality control on the 1/10° grid revealed more outliers than quality control on the coarser grids, thereby improving data quality. During objective analysis, radius of influence was adjusted in accordance with grid size (Table 1), allowing the fine structure of the gridded fields to be revealed, especially in areas with sharp gradients of temperature and salinity such as fronts and river plumes.

The below maps illustrate large-scale and meso-scale features in temperature and salinity fields. Features such as river plumes and fronts are clearly visible at the 1/10° resolution, making the 1/10° climatology especially valuable for high-resolution ocean modeling and other applications.

Figure 4.1 is a comparison of 1°, 1/4° and 1/10° resolution maps of annual temperature at the surface. The Polar Front in the Sea of Japan is clearly visible at 1/10° resolution but almost indistinct at 1/4° resolution. Two major fronts stand out at 1/10° resolution: the Polar Front that cuts across the Sea of Japan, and Kuroshio Front between Taiwan and Japan. The Polar Front is distinct in the 1/10° resolution map year round, being best seen in winter (Figure 4.3).

The Kuroshio Front stands out in seasonal maps of SST for winter and spring as a high-gradient band extending northeast of Taiwan toward Japan (Figure 4.3). In summer, the Kuroshio Front is barely seen as the summer warming makes SST spatially uniform and SST gradient across the Kuroshio vanishes (Hickox *et al.*, 2000). In fall, the cross-frontal SST gradient strengthens, so that the Kuroshio Front becomes clearly visible.

Tidal mixing fronts in the Yellow Sea are distinct in the wintertime 1/10° resolution map of SST (Figure 4.3). These fronts are observed off the Shandong Peninsula, Jiangsu Shoal, Seohan Bay, and Kyunggi Bay and are named by Hickox *et al*. (2000) after these coastal and bathymetric features (Figure 2.3).

In the Seto Inland Sea (centered at 34°10′N, 133°20′E), north-south gradients of SST and sea surface salinity (SSS) are resolved in 1/10° seasonal maps (Figure 4.3 and Figure 4.4), and not resolved in the 1/4° and 1° seasonal maps (not shown). Temperature and salinity along the northern shore of the Seto Inland Sea are, respectively, colder and fresher than those along its southern shores where the Seto Inland Sea is connected to the open ocean.

Figure 4.2 is a comparison of the 1°, 1/4°, and 1/10° resolution maps of annual SSS, while Figure 4.4 presents seasonal maps of SSS at 1/10° resolution. The 1/10° maps of SSS are especially useful as they reveal several individual river outflows that are not resolved (or poorly resolved) at lower resolutions. The Yangtze River (Changjiang River, CR) outflow stands out in all maps thanks to this outflow's sheer size, which is commensurate with the Yangtze River discharge. The Min River (MR) outflow to the East China Sea at 26°N is only resolved at 1/10° resolution. West of Korea, two low-salinity areas are maintained by the discharges of Han River (HR) and Taedong River (TR). In the Bohai Sea, two areas of low salinity are revealed. The low salinity in the southwestern Bohai Sea is caused by the discharge of several rivers, particularly the Yellow River (YR). The freshening of the northeastern Bohai Sea is caused by the discharge of rivers belonging to the Liaohe River (LR) basin.

The Yangtze River Diluted Water (YRDW) formed by mixing of the Yangtze River outflow with offshore water can be clearly seen in all four seasonal maps. The shape, orientation, and salinity of YRDW change seasonally (Figure 4.4) depending on monsoon winds and Yangtze River discharge. In winter, due to the decreased discharge of the Yangtze River, the extent of YRDW is limited. In spring and summer, the Yangtze River discharge increases sharply; as a result, the YRDW protrudes east and northeast. In fall, the YRDW extends southward along China's coast into Taiwan Strait. The southward propagation of YRDW is facilitated by the northerly winds associated with the winter monsoon (Ichikawa and Beardsley, 2002).

The seasonal development of the Yellow Sea Cold Water Mass (e.g., Zhang *et al*., 2008) can be clearly seen in our climatologies with 1°, 1/4°, and 1/10° resolution (Figure 4.5) that show this water mass at the same location and with the same temperature as revealed by synoptic ship-borne observations (Zhang *et al*., 2008). Our 1/10° resolution maps provide the best depiction of this water mass.

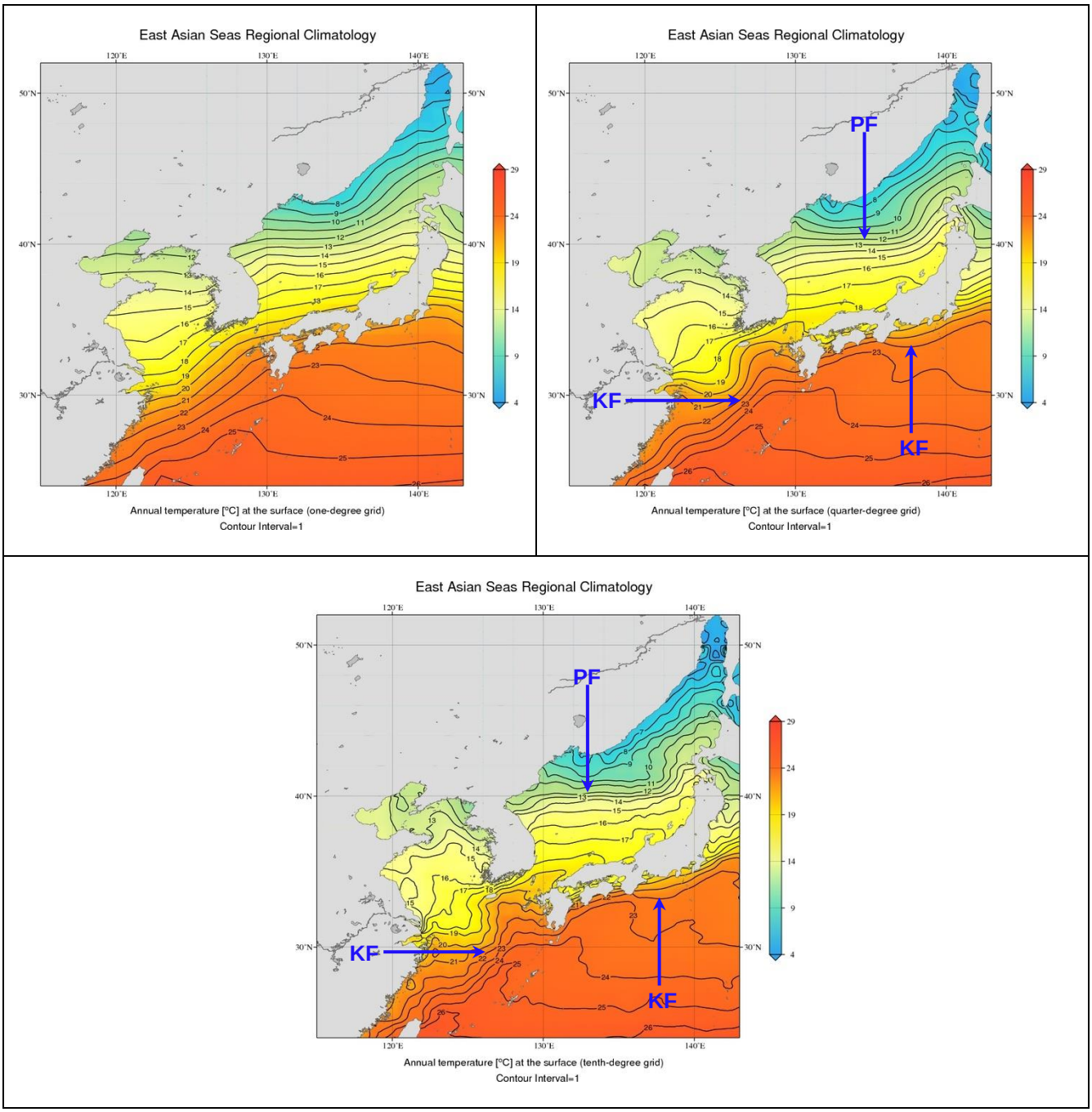

Figure 4.1. Comparison of annual SST on three grids: 1° (left) *vs.* 1/4° (right) *vs.* 1/10° (bottom). Acronyms: KF, Kuroshio Front; PF, Polar Front.

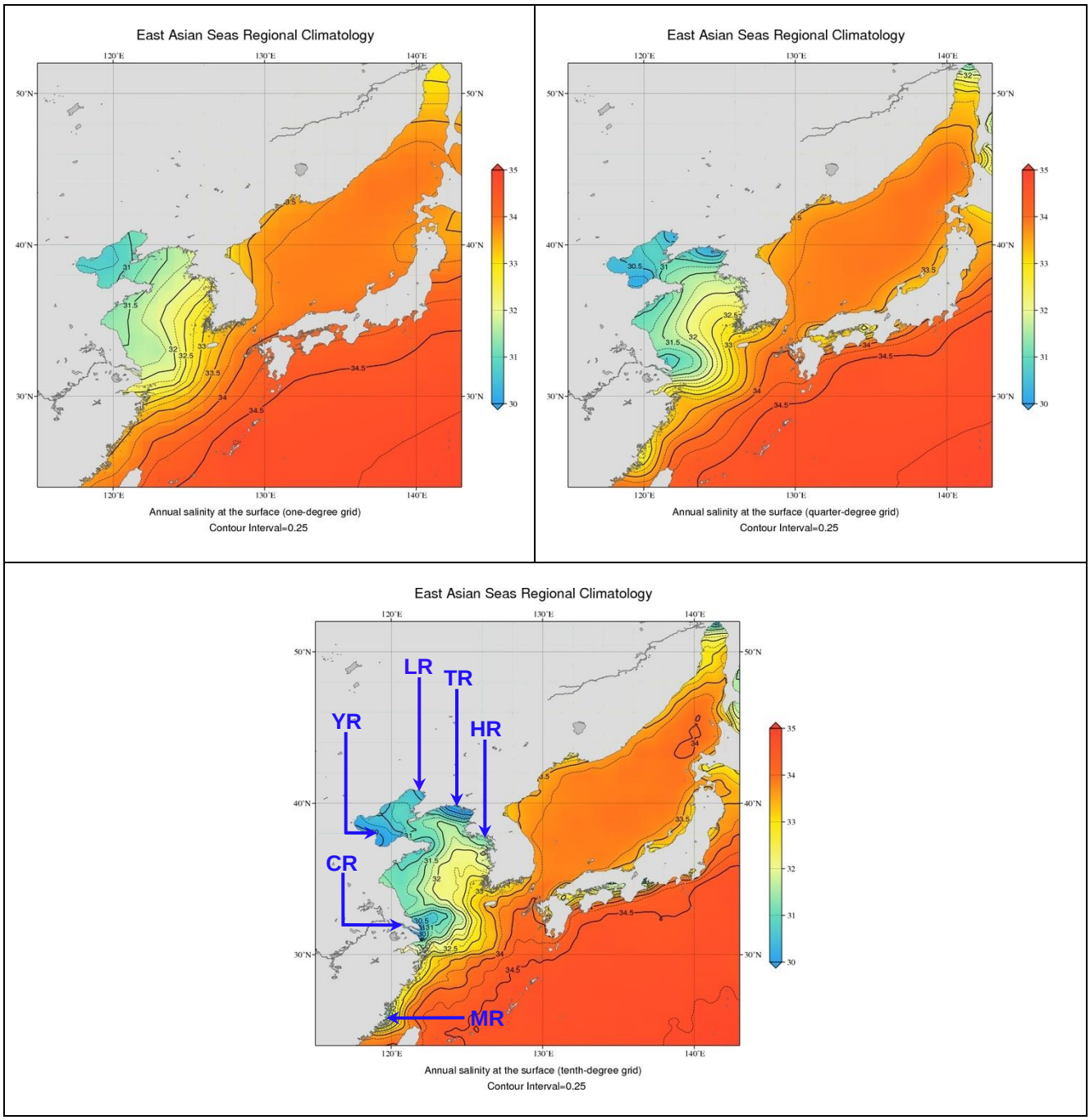

Figure 4.2. Comparison of annual SSS on three grids: 1° (left) *vs.* 1/4° (right) *vs.* 1/10° (bottom). Acronyms: CR, Yangtze (Changjiang) River; HR, Han River; LR, Liaohe River; MR, Min River; TR, Taedong River; YR, Yellow River.

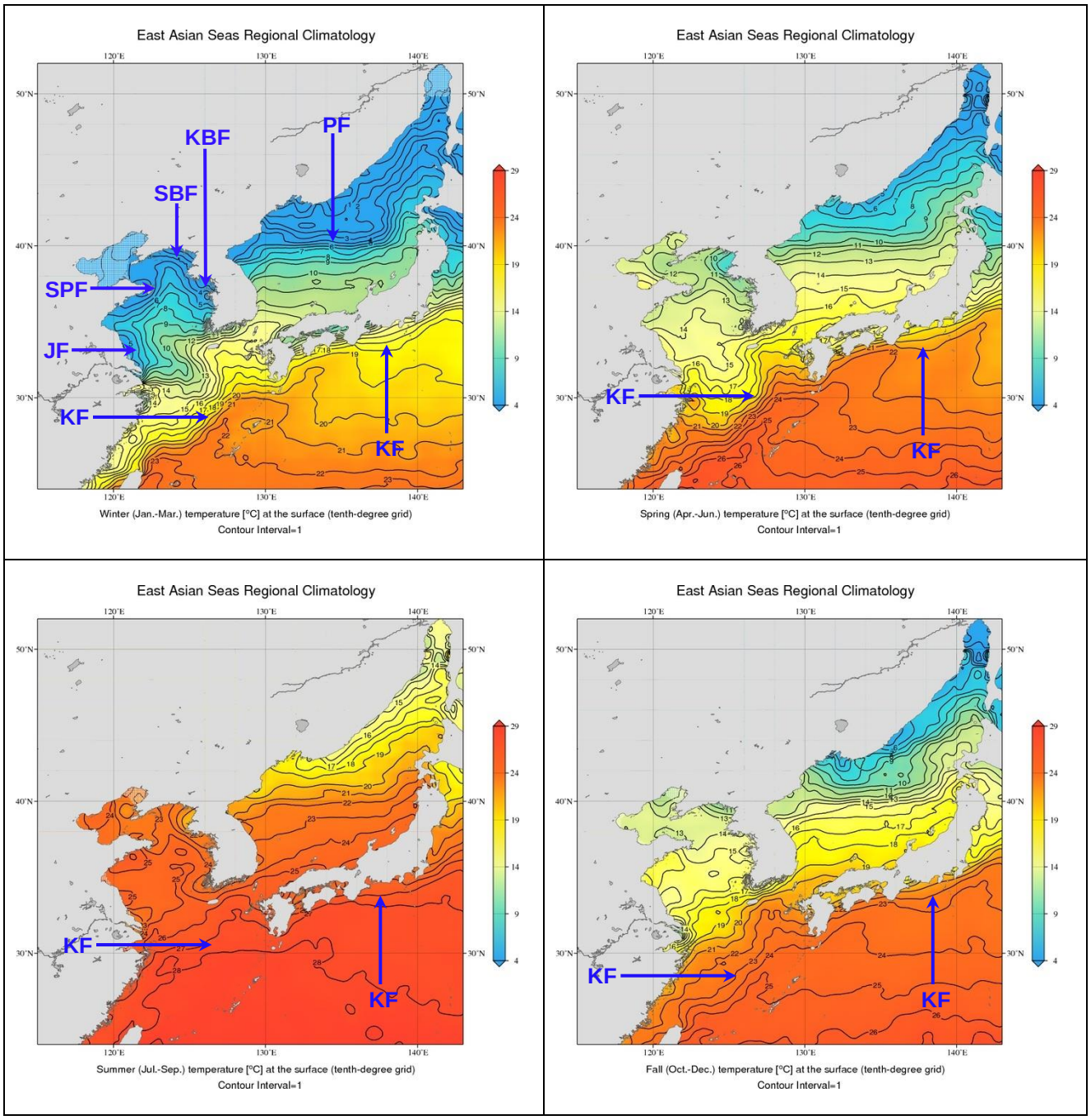

Figure 4.3. Seasonal maps of SST on the 1/10° grid. Seasons are: winter (January-March), spring (April-June), summer (July-September), and fall (October-December). Labeled are major large-scale and meso-scale fronts. Acronyms: JF, Jiangsu Front; KBF, Kyunggi Bay Front; KF, Kuroshio Front; PF, Polar Front; SBF, Seohan Bay Front; SPF, Shandong Peninsula Front (Hickox *et al.*, 2000).

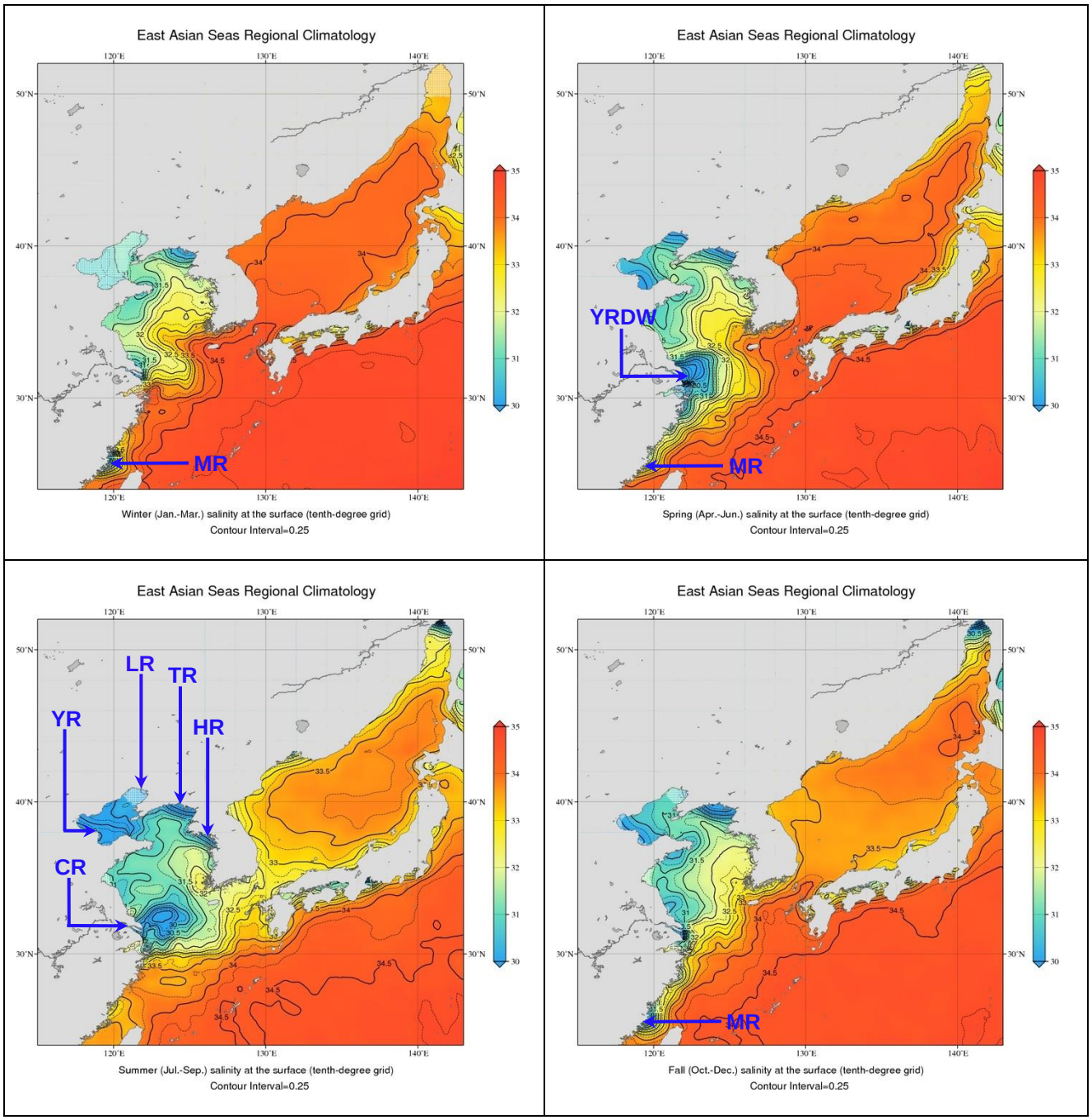

Figure 4.4. Seasonal maps of SSS on 1/10° grid. Seasons are: winter (January-March), spring (April-June), summer (July-September), and fall (October-December). Labeled are outflows of major rivers. Acronyms: CR, Yangtze (Changjiang) River; HR, Han River; LR, Liaohe River; MR, Min River; TR, Taedong River; YR, Yellow River; YRDW, Yangtze River Diluted Water.

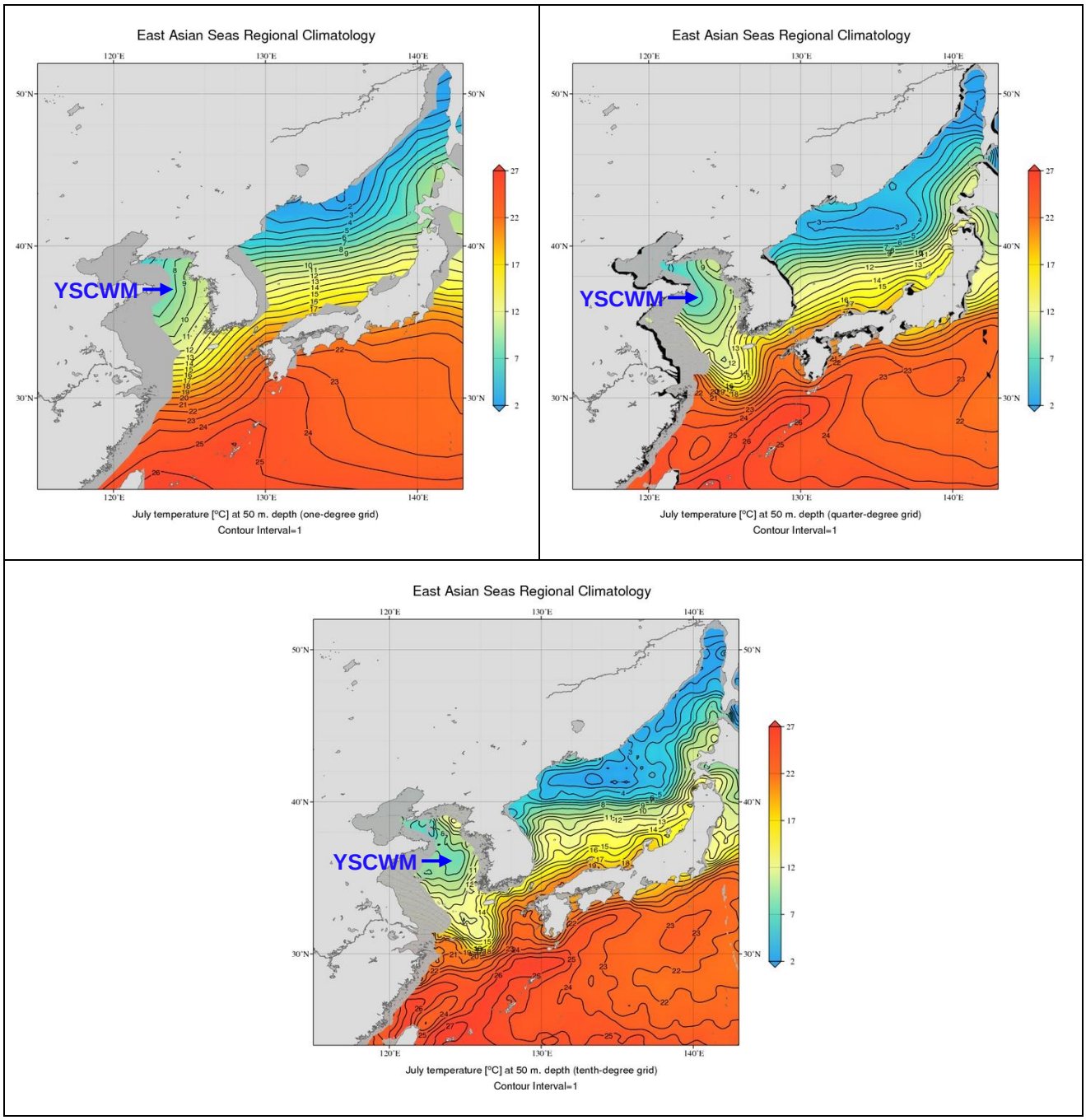

Figure 4.5. Temperature [°C] at 50 m depth (T50) in July. YSCWM, Yellow Sea Cold Water Mass. Comparison of T50 at three resolutions (1° (left) *vs.* 1/4° (right) *vs.* 1/10° (bottom)) shows that the YSCWM is more realistic in the 1/10° resolution map.

The Kuroshio Front (Figure 4.6) is the most robust feature in the East China Sea.

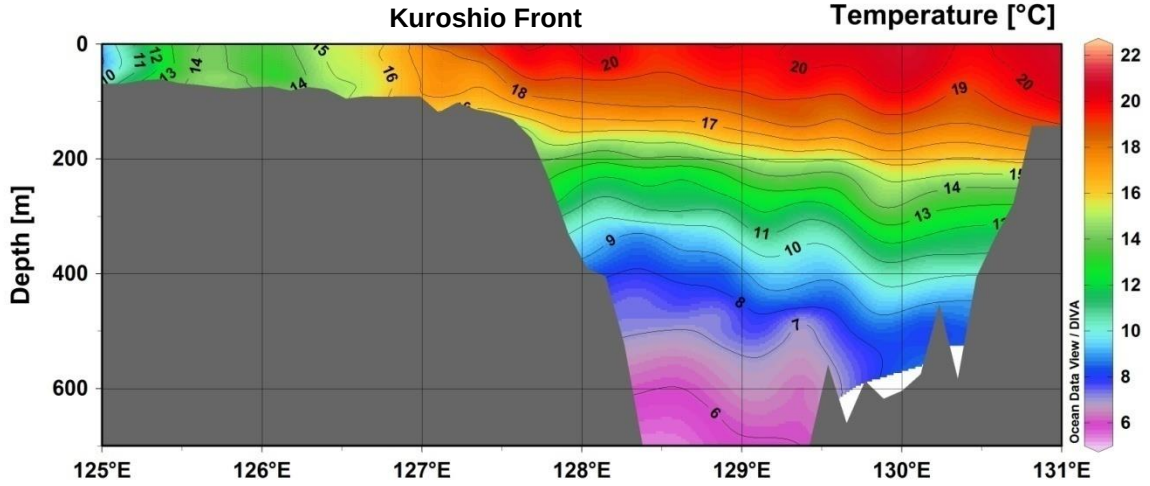

Figure 4.6. Winter temperature vertical section along 30.125°N across the Kuroshio Front. Based on the EAS Regional Climatology statistical mean gridded 1/4° data.

The Yellow Sea Cold Water Mass (YSCWM) is found in the central part of the Yellow Sea below the thermocline (Figure 4.7).

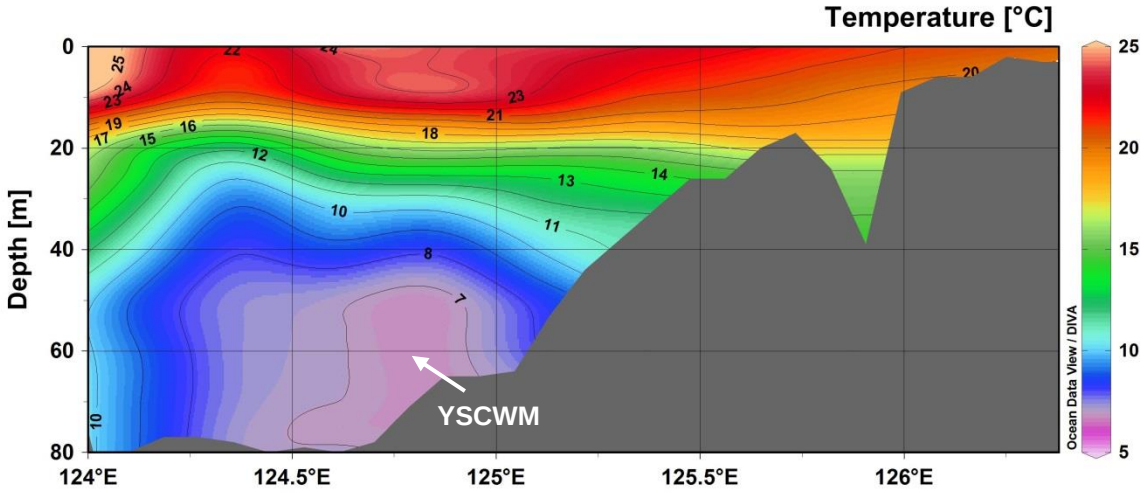

Figure 4.7. July temperature vertical section along 36.375°N showing the Yellow Sea Cold Water Mass (YSCWM). Based on the EAS Regional Climatology statistical mean gridded 1/4° data.

The Polar Front is the most robust feature in the Sea of Japan. It is shown in the winter temperature vertical section along 135.125°E (Figure 4.8).

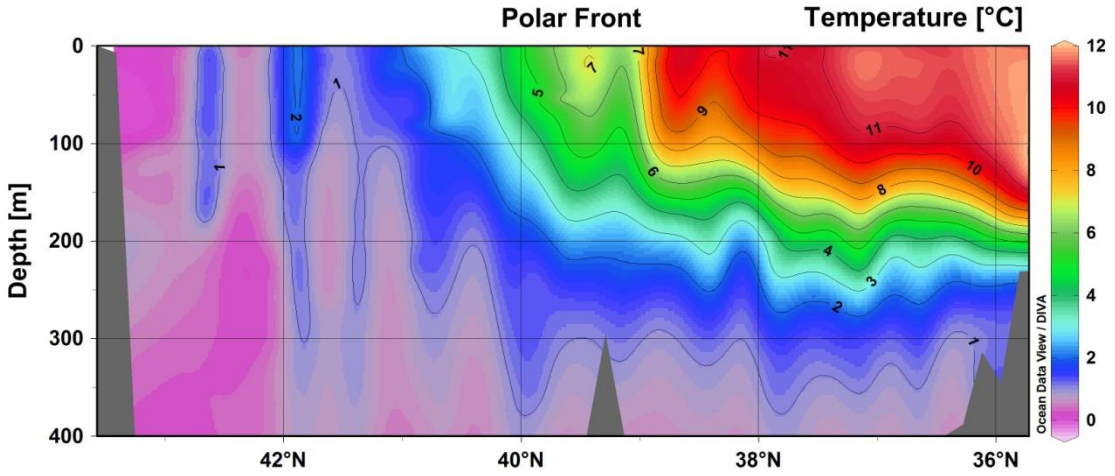

Figure 4.8. Winter temperature vertical section along 135.125°E across the Polar Front. Based on the EAS Regional Climatology statistical mean gridded 1/4° data.

The Kuroshio Front in the Northwest Pacific Ocean south of Honshu is shown in the winter temperature vertical section along 135.875°E (Figure 4.9).

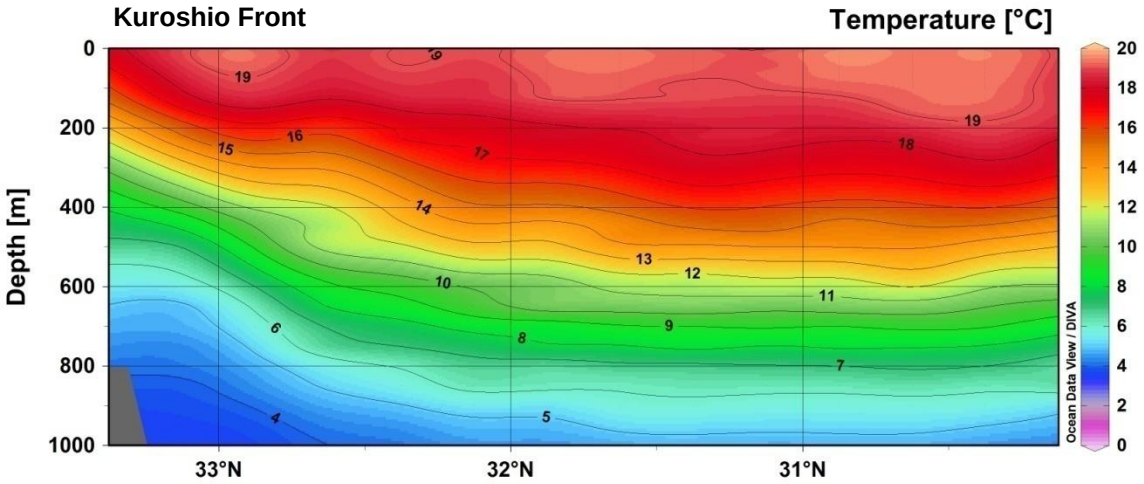

Figure 4.9. Winter temperature vertical section along 135.875°E across the Kuroshio Front. Based on the EAS Regional Climatology statistical mean gridded 1/4° data.

5. AVAILABILITY OF MAPS AND DATA

Available are seven types of long-term annual, seasonal and monthly data sets and attendant maps at standard levels, at 1°, 1/4°, and 1/10° resolution, for temperature and salinity:

(1) Objectively analyzed climatologies. The objectively interpolated mean fields based on 1°, 1/4°, and 1/10° grids.

(2) Statistical mean climatologies. The average of all unflagged values in each grid cell containing at least one measurement.

(3) Number of observations in each grid cell.

(4) Standard deviation in each grid cell.

(5) Standard error of the mean in each grid cell.

(6) Seasonal or monthly climatology minus the annual climatology in each grid cell.

(7) Statistical mean minus the climatological mean in each grid cell.

5.1 MAPS

Maps can be viewed on the EAS Regional Climatology webpage. All maps were generated using the Generic Mapping Tools (GMT; Wessel and Smith, 1998). The bathymetry in these maps is ETOPO-based: the mean depth value within each grid cell was calculated from ETOPO2 (National Geophysical Data Center, 2006) for the 1° and 1/4° maps and from ETOPO1 (Amante and Eakins, 2009) for the 1/10° maps.

5.2 GRIDDED DATA

The objectively-analyzed and statistical mean fields can be obtained in comma-separated value (CSV), ArcGIS, and netCDF formats from the EAS Regional Climatology webpage.

5.3 UNGRIDDED DATA

The ungridded quality-controlled data can be retrieved using World Ocean Database Select (an online search and retrieval interface). The user can download either observed level data or standard level data obtained by vertical interpolation of observed data onto a set of standard levels described in World Ocean Database 2013 User's Manual (Johnson *et al.*, 2013). Data are available as ASCII, comma separated value (CSV), and netCDF formats.

6. SUMMARY

The East Asian Seas Regional Climatology documents spatial and temporal distribution of temperature and salinity on 1°, 1/4°, and 1/10° grids, computed by objective analysis of quality-controlled data from the World Ocean Database 2013. High-resolution climatologies reveal numerous meso-scale features, *e.g.*, water masses, fronts, and river plumes. These features are validated by comparing them with *in situ* observations reported in the oceanographic literature. The feature-based approach is thus shown to be a powerful instrument for validation of regional climatologies. As more data are received, we will be updating our analysis when such updates are justified by the volume of additional observations. In particular, we plan to build a set of climatological analyses for oxygen, nutrients, and other essential oceanographic parameters, thereby providing a basis for future releases of updated and enhanced versions of the East Asian Seas Regional Climatology.

7. ACKNOWLEDGMENTS

We are thankful to the NCEI for support during the preparation of this paper. We thank the NIFS for their collaboration on the EAS Regional Climatology. We acknowledge Joon-Soo Lee (NIFS) for his assistance with quality control during the preparation of the EAS Regional Climatology.

We acknowledge the contribution of numerous individuals, organizations, and countries, for the submission of data included in the EAS Regional Climatology. Many previously unavailable data were identified and rescued as a result of the IOC/IODE Global Oceanographic

Data Archaeology and Rescue (GODAR) project initiated and led by Sydney Levitus, and the IOC/IODE World Ocean Database (WOD) project. At NCEI/WDC, data archaeology and rescue projects were supported with funding from the NOAA National Environmental Satellite, Data, and Information Service (NESDIS) and the NOAA Climate Program Office.

Maps were created using the Generic Mapping Tools (GMT) software developed by Paul Wessel, University of Hawaii, and Walter H.F. Smith, NOAA. Vertical sections were created using the Ocean Data View (ODV) software developed by Reiner Schlitzer, Alfred Wegener Institute for Polar and Marine Research.

We acknowledge the scientists, technicians, and programmers who collected and processed data, those individuals who submitted data to national and regional data centers as well as the managers and staff at the various data centers. We thank our colleagues at the NCEI and NIFS. Their efforts have made this work possible. We extend our most sincere gratitude to all.

We also gratefully acknowledge the reviewers (Igor Belkin, University of Rhode Island; Robert Helber, Naval Research Laboratory; Ricardo Locarnini, NCEI; Charles Sun, NCEI), editor (Dan Seidov, NCEI), and technical editor (Alexey Mishonov, NCEI), whose thoughtful comments significantly contributed to the improvement of this paper.

8. REFERENCES

Amante, C., Eakins, B.W., 2009. ETOPO1 1 Arc-Minute Global Relief Model: Procedures, Data Sources and Analysis. NOAA Technical Memorandum NESDIS NGDC-24. National Geophysical Data Center, NOAA. DOI:10.7289/V5C8276M.

Beardsley, R.C., Limeburner, R., Yu, H., Cannon, G.A., 1985. Discharge of the Changjiang (Yangtze River) into the East China Sea. Continental Shelf Research 4 (1-2), 57-76. DOI: 10.1016/0278-4343(85)90022-6.

Belkin, I.M., 2002a. East China Sea. In: James W. Nybakken, William W. Broenkow, and Tracy L. Vallier (Eds.), Interdisciplinary Encyclopedia of Marine Sciences, Volume 1, 334-335. Grolier Academic Reference, Danbury, Conn.

Belkin, I.M., 2002b. Yellow Sea. In: James W. Nybakken, William W. Broenkow, and Tracy L. Vallier (Eds.), Interdisciplinary Encyclopedia of Marine Sciences, Volume 3, 365-366. Grolier Academic Reference, Danbury, Conn.

Belkin, I.M., Krishfield, R., Honjo, S., 2002. Decadal variability of the North Pacific Polar Front: Subsurface warming versus surface cooling. Geophysical Research Letters 29 (9), 1351. DOI: 10.1029/2001GL013806.

Belkin, I.M., Cornillon, P., 2003. SST fronts of the Pacific coastal and marginal seas. Pacific Oceanography 1 (2), 90-113.

Belkin, I.M., Cornillon, P.C., Sherman, K., 2009. Fronts in Large Marine Ecosystems. Progress in Oceanography 81 (1-4), 223-236.

Boyer, T.P., Levitus, S., Garcia, H.E., Locarnini, R.A., Stephens, C., Antonov, J.I., 2005. Objective analyses of annual, seasonal, and monthly temperature and salinity for the world ocean on a 0.25 degree grid. International Journal of Climatology, 25 (7), 931-945.

Boyer, T.P., Biddle, M., Hamilton, M., Mishonov, A.V., Paver, C., Seidov, D., Zweng, M., 2015. Gulf of Mexico Regional Climatology, NOAA/NODC, available at http://dx.doi.org/10.7289/V5C53HSW.

Boyer, T.P., Baranova, O.K., Biddle, M., Johnson, D.R., Mishonov, A.V., Paver, C., Seidov, D., Zweng, M., 2012. Arctic Regional Climatology, Regional Climatology Team, NOAA/NODC, www.nodc.noaa.gov/OC5/regional_climate/arctic.

Boyer, T.P., Antonov, J.I., Baranova, O.K., Coleman, C., Garcia, H.E., Grodsky, A., Johnson, D.R., Locarnini, R.A., Mishonov, A.V., O'Brien, T.D., Paver, C.R., Reagan, J.R., Seidov, D., Smolyar, I.V., Zweng, M.M., 2013. World Ocean Database 2013, *NOAA Atlas NESDIS 72*, S. Levitus, Ed., A. Mishonov, Technical Ed.; Silver Spring, MD, 209 pp.

Chen, C.-T.A., 2009. Chemical and physical fronts in the Bohai, Yellow and East China seas. Journal of Marine Systems 78 (3), 394-410. DOI:10.1016/j.jmarsys.2008.11.016.

Choi, Y.-K., 1996. Open-ocean convection in the Japan (East) Sea. La Mer 34, 259–272.

Fang, G., Zhao, B., Zhu, Y., 1991. Water volume transport through the Taiwan Strait and the continental shelf of the East China Sea measured with current meters. In: Oceanography of Asian Marginal Seas, edited by K. Takano. Elsevier, New York, pp. 345-348.

Gamo, T., Nozaki, Y., Sakai, T., Nakai, T., Tsubota, H., 1986. Spacial and temporal variations of water characteristics in the Japan Sea bottom layer. Journal of Marine Research 44 (4), 781-793. DOI: 10.1357/002224086788401620.

Hickox, R., Belkin, I., Cornillon, P., Shan, Z., 2000. Climatology and seasonal variability of ocean fronts in the East China, Yellow and Bohai seas from satellite SST data. Geophysical Research Letters 27 (18), 2945-2948. DOI: 10.1029/1999GL011223.

Hogan, P.J., Hurlburt, H.E., 2006. Why do intrathermocline eddies form in the Japan/East Sea? A modeling perspective. Oceanography 19 (3), 134-143. DOI: 10.5670/oceanog.2006.50.

Ichikawa, H., Beardsley, R.C., 2002. The current system in the Yellow and East China Seas. Journal of Oceanography 58 (1), 77-92. DOI: 10.1023/A:1015876701363.

Imawaki, S., Bower, A.S., Beal, L., Qiu, B., 2013. In: Gerold Siedler, Stephen M. Griffies, W. John Gould, and John Church (Eds.), Ocean Circulation and Climate - a 21st Century Perspective, 2nd Edition, pp. 305-338. Elsevier - Academic Press, Amsterdam.

International Hydrographic Organization, 1953. Limits of Oceans and Seas, 3rd edition, Special Publication No. 23, Monaco, 42 pp.

Isobe, A., 2008. Recent advances in ocean-circulation research on the Yellow Sea and East China Sea shelves. Journal of Oceanography 64 (4), 569-584. DOI: 10.1007/s10872-008-0048-7.

Isoda, Y., Saitoh, S., Mihara, M., 1991. SST structure of the Polar Front in the Japan Sea. In: Oceanography of Asian Marginal Seas, edited by K. Takano. Elsevier, New York, pp. 103-112.

Jan, S., Wang, J., Chern, C.-S., Chao, S.-Y., 2002. Seasonal variation of the circulation in the Taiwan Strait. Journal of Marine Systems 35 (3-4), 249-268. DOI: 10.1016/S0924-7963(02)00130-6.

Johnson, D.R., Boyer, T.P., 2015. East Asian Seas Regional Climatology (Version 2). National Centers for Environmental Information, NOAA, USA. DOI: 10.7289/V5MP5171.

Johnson, D.R., Boyer, T.P., Garcia, H.E., Locarnini, R.A., Baranova, O.K., Zweng, M.M., 2013. World Ocean Database 2013 User's Manual. Ed. S. Levitus. *NODC Internal Report 22*, Silver Spring, MD, 172 pp. DOI:10.7289/V5DF6P53.

Kawai, H., 1998. A brief history of recognition of the Kuroshio. Progress in Oceanography 41(4), 505-578. DOI: 10.1016/S0079-6611(98)00024-X.

Kim, K., Kim, K.-R., Kim, Y.-G., Cho, Y.-K., Kang, D.-J., Takematsu, M., Volkov, Y., 2004. Water masses and decadal variability in the East Sea (Sea of Japan). Progress in Oceanography 61 (2-4), 157-174. DOI: 10.1016/j.pocean.2004.06.003.

Kim, Y.J., 2007. A study on the Japan/East Sea oceanic circulation using an extra-fine resolution model. Ph.D. thesis, Interdisciplinary Graduate School of Engineering Sciences, Kyushu University.

Kondo, M., 1985. Oceanographic investigations of fishing grounds in the East China Sea and the Yellow Sea – Part 1: Characteristics of the mean temperature and salinity distributions measured at 50 m and near the bottom. Bulletin of the Seikai Regional Fisheries Research Laboratory 62, 19-55 (in Japanese with English abstract).

KORDI (Korea Ocean Research and Development Institute), 1987. Oceanographic Atlas of Korean Waters, Volume 1, Yellow Sea. KORDI, 147 pp.

Li, P., Yang, S.L., Milliman, J.D., Xu, K.H., Qin, W.H., Wu, C.S., Chen, Y.P., Shi, B.W., 2012. Spatial, temporal, and human-induced variations in suspended sediment concentration in the surface waters of the Yangtze Estuary and adjacent coastal areas. Estuaries and Coasts 35 (5), 1316-1327. DOI: 10.1007/s12237-012-9523-x.

Lie, H.-J., Cho, C.-H., 1994. On the origin of the Tsushima Warm Current. Journal of Geophysical Research-Oceans 99 (C12), 25081-25091. DOI: 10.1029/94JC02425.

Lin, X., Xie, S.-P., Chen, X., Xu, L., 2006. A well-mixed warm water column in the central Bohai Sea in summer: Effects of tidal and surface wave mixing. Journal of Geophysical Research 111 (C11), Article C11017. DOI: 10.1029/2006JC003504.

Locarnini, R.A., Mishonov, A.V., Antonov, J.I., Boyer, T.P., Garcia, H.E., Baranova, O.K., Zweng, M.M., Paver, C.R., Reagan, J.R., Johnson, D.R., Hamilton, M., Seidov, D., 2013. World Ocean Atlas 2013, Vol. 1: Temperature. S. Levitus, Ed: A. Mishonov, Technical Ed. NOAA Atlas NESDIS 73, 40 pp.

Mao, X., Jiang, W., Zhao, P., Gao, H., 2008. A 3-D numerical study of salinity variations in the Bohai Sea during the recent years. Continental Shelf Research 28 (19), 2689-2699. DOI: 10.1016/j.csr.2008.09.004.

Martin, S., Kawase, M., 1998. The southern flux of sea ice in the Tatarskiy Strait, Japan Sea and the generation of the Liman Current. Journal of Marine Research 56 (1), 141-155. DOI: 10.1357/002224098321836145.

Matsuno, T., Lee, J.-S., Yanao, S., 2009. The Kuroshio exchange with the South and East China Seas. Ocean Science 5 (3), 303-312.

Menard, H.W., Smith, S.M., 1966. Hypsometry of ocean basin provinces. Journal of Geophysical Research 71 (18), 4305-4325.

Milliman, J.D., Meade, R.H., 1983. World-wide delivery of river sediment to the oceans. Journal of Geology 91 (1), 1-21.

National Geophysical Data Center, 2006. U.S. Department of Commerce, National Oceanic and Atmospheric Administration, *2-minute Gridded Global Relief Data (ETOPO2v2)* http://www.ngdc.noaa.gov/mgg/fliers/06mgg01.html.

Niino, H., Emery, K.O., 1961. Sediments of shallow portions of East China Sea and South China Sea. Geological Soc. of America Bull., 72, 731–762.

Nitani, H., 1972. On the deep and bottom waters in the Japan Sea. In: Research in Hydrography and Oceanography, edited by D. Shoji. Hydrographic Department of Japan, Tokyo, pp. 159-201.

Nof, D., 2001. China's development could lead to bottom water formation in the Japan/East Sea. Bulletin of the American Meteorological Society 82 (4), 609-618. DOI: 10.1175/1520-0477(2001)082<0609:CDCLTB>2.3.CO;2.

Qiu, B., 2001. Kuroshio and Oyashio currents. In: Encyclopedia of Ocean Sciences, Volume 3, edited by John H. Steele, Karl K. Turekian, and Steve A. Thorpe. Academic Press, New York, pp. 1413-1425. DOI: 10.1006/rwos.2001.0350.

Seidov, D., Baranova, O.K., Biddle, M., Boyer, T.P., Johnson, D.R., Mishonov, A.V., Paver, C., Zweng, M., 2013. Greenland-Iceland-Norwegian Seas Regional Climatology, Regional Climatology Team, NOAA/NODC, available at http://dx.doi.org/10.7289/V5GT5K30.

Seidov, D., Baranova, O.K., Boyer, T.P., Johnson, D.R., Mishonov, A.V., Parsons, A.R. 2015. Northwest Atlantic Regional Climatology, Regional Climatology Team, NOAA/NCEI (www.nodc.noaa.gov/OC5/regional_climate/nwa-climate).

Senjyu, T., Sudo, H., 1993. Water characteristics and circulation of the upper portion of the Japan Sea Proper Water. Journal of Marine Systems 4 (4), 349-362. DOI: 10.1016/0924-7963(93)90029-L.

Senjyu, T., Sudo, H., 1994. The upper portion of the Japan Sea Proper Water; Its source and circulation as deduced from isopycnal analysis. Journal of Oceanography 50 (6), 663-690.

Senjyu, T., 1999. The Japan Sea Intermediate Water; its characteristics and circulation. Journal of Oceanography 55 (2), 111-122. DOI: 10.1023/A:1007825609622.

Senjyu, T., Enomoto, H., Matsuno, T., Matsui, S., 2006. Interannual salinity variations in the Tsushima Strait and its relation to the Changjiang discharge. Journal of Oceanography 62 (5), 681-692. DOI: 10.1007/s10872-006-0086-y.

Seung, Y.-H., Yoon, J.-H., 1995. Some features of winter convection in the Japan Sea. Journal of Oceanography 51 (1), 61-73. DOI: 10.1007/BF02235936.

Shen, F., Zhou, Y.X., Li, J.F., He, Q., Verhoef, W., 2013. Remotely sensed variability of the suspended sediment concentration and its response to decreased river discharge in the Yangtze estuary and adjacent coast. Continental Shelf Research 69, 52-61. DOI:

10.1016/j.csr.2013.09.002.

Su, H., Wang, Y., 2012. Using MODIS data to estimate sea ice thickness in the Bohai Sea (China) in the 2009-2010 winter. Journal of Geophysical Research-Oceans 117 (C10), Article C10018. DOI: 10.1029/2012JC008251.

Su, J., 1998. Circulation dynamics of the China Seas north of 18°N. In: The Global Coastal Ocean, Volume 11: Regional Studies and Syntheses, edited by A.R. Robinson and K.H. Brink. New York, John Wiley & Sons, pp. 483-505.

Sudo, H., 1986. A note on the Japan Sea Proper Water. Progress in Oceanography 17 (3-4), 313-336. DOI: 10.1016/0079-6611(86)90052-2.

Talley, L.D., Lobanov, V., Ponomarev, V., Salyuk, A., Tishchenko, P., Zhabin, I., Riser, S., 2003. Deep convection and brine rejection in the Japan Sea. Geophysical Research Letters 30 (4), Article 1159. DOI: 10.1029/2002GL016451.

Talley, L., Min, D.-H., Lobanov, V.B., Luchin, V.A., Ponomarev, V.I., Salyuk, A.N., Shcherbina, P.Y., Tishchenko, P.Y., Zhabin, I., 2006. Japan/East Sea water masses and their relations to the sea's circulation. Oceanography 29 (3), 32-49. DOI: 10.5670/oceanog.2006.42.

Talley, L.D., Pickard, G.L., Emery, W.J, Swift, J.H., 2011. Descriptive Physical Oceanography: An Introduction, 6th edition. Elsevier, Boston, 560 pp.

Tang, D.L., Kawamura, H., Oh, I.S., Baker, J., 2006. Satellite evidence of harmful algal blooms and related oceanographic features in the Bohai Sea during autumn 1998. Advances in Space Research 37 (4), 681-689. DOI: 10.1016/j.asr.2005.04.045.

Taniguchi, M., Ishitobi, T., Chen, J.Y., Onodera, S.-I., Miyaoka, K., Burnett, W.C., Peterson, R., Liu, G.Q., Fukushima, Y., 2008. Submarine groundwater discharge from the Yellow River Delta to the Bohai Sea, China. Journal of Geophysical Research-Oceans 113 (C6), Article C06025. DOI: 10.1029/2007JC004498.

Teng, S.K., Yu, H., Tang, Y., Tong, L., Choi, C.I., Kang, D., Liu, H., Chun, Y., Juliano, R.O., Rautalahti-Miettinen, E., Daler, D., 2005. Yellow Sea. Global International Waters Assessment (GIWA) Regional Assessment 34. University of Kalmar on behalf of United Nations Environment Programme, Kalmar, Sweden, 114 pp.

Uda, M., 1934. The results of simultaneous oceanographic investigations in the Japan Sea and its adjacent waters in May and June 1932. Journal of the Imperial Fisheries Experimental Station 5, 57-190.

Uda, M., 1936. Results of simultaneous oceanographic investigations in the Japan Sea and its adjacent waters during October and November, 1933. Journal of the Imperial Fisheries Experimental Station, 7, 91–151 (in Japanese).

Wang, Q., Guo, X.Y., Takeoka, H., 2008. Seasonal variations of the Yellow River plume in the Bohai Sea: A model study. Journal of Geophysical Research-Oceans 113 (C8), Article C08046, 1-14. DOI: 10.1029/2007JC004555.

Wessel, P., Smith, W.F., 1998. New, improved version of Generic Mapping Tools released. Eos, Transactions of the American Geophysical Union 79 (47), 579.

Wu, B.Y., Wang, J., 2002. Winter Arctic Oscillation, Siberian High and East Asian winter monsoon. Geophysical Research Letters 29 (19), Article 1897. DOI: 10.1029/2002GL015373.

Yang, S.L., Liu, Z., Dai, S.B., Gao, Z.X., Zhang, J., Wang, H.J., Luo, X.X., Wu, C.S., Zhang, Z., 2010. Temporal variations in water resources in the Yangtze River (Changjiang) over the Industrial Period based on reconstruction of missing monthly discharges. Water Resources Research 46, Article W10516. DOI: 10.1029/2009WR008589.

Yang, S.L., Milliman, J.D., Xu, K.H., Deng, B., Zhang, X.Y., Luo, X.X., 2014. Downstream sedimentary and geomorphic impacts of the Three Gorges Dam on the Yangtze River. Earth-Science Reviews 138, 469-486. DOI: 10.1016/j.earscirev.2014.07.006.

Yang, S.L., Xu, K.H., Milliman, J.D., Yang, H.F., Wu, C.S., 2015. Decline of Yangtze River water and sediment discharge: Impact from natural and anthropogenic changes. Scientific Reports 5, 12581. DOI: 10.1038/srep12581.

Yoon, J.-H., 1982. Numerical experiment on the circulation in the Japan Sea. Part I. Formation of the East Korean Warm Current. Journal of the Oceanographical Society of Japan 38, 43-51.

Yoon, J.-H., Kim, Y-J., 2009. Review on the seasonal variation of the surface circulation in the Japan/East Sea. Journal of Marine Systems 78 (2), 226-236. DOI: 10.1016/j.jmarsys.2009.03.003.

Yoshikawa, Y., Awaji, T., Akitomo, K., 1999. Formation and circulation processes of intermediate water in the Japan Sea. Journal of Physical Oceanography 29 (8), 1701-1722. DOI: 10.1175/1520-0485(1999)029<1701:FACPOI>2.0.CO;2.

Yu, Y.G., Wang, H.J., Shi, X.F., Ran, X.B., Cui, T.W., Qiao, S.Q., Liu, Y.G., 2013. New discharge regime of the Huanghe (Yellow River): Causes and implications. Continental Shelf Research 69, 62-72. DOI: 10.1016/j.csr.2013.09.013.

Yuan, S.A., Gu, W., Xu, Y.J., Wang, P., Huang, S.Q, Le, Z.Y., Cong, J.O., 2012. The estimate of sea-ice resources quantity in the Bohai Sea based on NOAA/AVHRR data. Acta Oceanologica Sinica 31 (1), 33-40. DOI: 10.1007/s13131-012-0173-4.

Zhang, S.W., Wang., Q.Y., Lu., Y., Cui, H., Yuan, Y.L., 2008. Observation of the seasonal evolution of the Yellow Sea Cold Water Mass in 1996-1998. Continental Shelf Research 28, 442-457. DOI: 10.1016/j.csr.2007.10.002.

Zweng, M.M., Reagan, J.R., Antonov, J.I., Locarnini, R.A., Mishonov, A.V., Boyer, T.P., Garcia, H.E., Baranova, O.K., Johnson, D.R., Seidov, D., Biddle, M.M., 2013. World Ocean Atlas 2013, Volume 2: Salinity. S. Levitus, Ed.; A. Mishonov, Technical Ed.. NOAA Atlas NESDIS 74, 39 pp.

This page intentionally left blank